Calcolo (2020) 57:2
https://doi.org/10.1007/s10092-019-0351-2

Ultra-weak symmetry of stress for augmented mixed finite element formulations in continuum mechanics

Javier A. Almonacid[1,2] · **Gabriel N. Gatica**[3] · **Ricardo Ruiz-Baier**[4,5]

Received: 28 June 2019 / Revised: 21 October 2019 / Accepted: 27 November 2019

Abstract
In this paper we propose a novel way to prescribe weakly the symmetry of stress tensors in weak formulations amenable to the construction of mixed finite element schemes. The approach is first motivated in the context of solid mechanics (using, for illustrative purposes, the linear problem of linear elasticity), and then we apply this technique to reduce the computational cost of augmented fully-mixed methods for thermal convection problems in fluid mechanics, in the case where several additional variables are defined. We show that the new approach allows to maintain the same structure of the mathematical analysis as in the original formulations. Therefore we only need to focus on ellipticity of certain bilinear forms, as this property provides feasible ranges for the stabilization parameters that complete the description of augmented methods. In addition, we present some numerical examples to show that these methods perform better than their counterparts that include vorticity, and emphasize that the reduction in degrees of freedom (and therefore, in computational cost) does not affect the quality of numerical solutions.

Keywords Mixed finite element methods · Ultra-weakly imposed symmetry · Linear elasticity · Boussinesq equations · A priori error estimates

Mathematics Subject Classification 65N30 · 74S05 · 76M10 · 65N15

This research was partially supported by CONICYT-Chile through the project AFB170001 of the PIA Program: Concurso Apoyo a Centros Científicos y Tecnológicos de Excelencia con Financiamiento Basal, and Fondecyt project 1161325; by Centro de Investigación en Ingeniería Matemática (CI^2MA), Universidad de Concepción; and by the Oxford Centre for Doctoral Training in Industrially Focused Mathematical Modelling.

✉ Gabriel N. Gatica
ggatica@ci2ma.udec.cl

Extended author information available on the last page of the article

Published online: 04 December 2019

1 Introduction

There is no doubt that the devise of numerical methods for problems in elastostatics and fluid mechanics is an active research area in Numerical Analysis (see, e.g., [2–4,14,18,19,21] and the references therein), and even when we have substantially different models for each of these areas (for instance, the linear elasticity and Navier–Stokes equations), one variable that is present in both contexts is the Cauchy stress $\boldsymbol{\sigma}$, a second order tensor that describes the state of stress at a point inside a material in the deformed state. In many applications $\boldsymbol{\sigma}$ is symmetric, and therefore, numerical methods must take into account this property. For the case of finite element methods, this is imposed either strongly (that is, the finite element is constructed in a way that only symmetric approximations are allowed) or weakly (that is via the corresponding variational formulation). In this work we focus on the latter.

A number of methods have been proposed to obtain acceptable approximations of the stress tensor. On the one hand, a common finite element to approximate the stress tensor is given by a row-wise approximation using Raviart–Thomas elements. Since this leads to an unsymmetric tensor, the symmetry is imposed weakly by considering this variable orthogonal to all skew-symmetric tensors, which then requires to introduce the vorticity tensor (the skew-symmetric part of the displacement gradient, or velocity gradient in the context of fluid mechanics) as an additional unknown. This idea, attributed to [17] and later formalized by [6,25], can provide asymptotically symmetric approximations for the stress, using fewer degrees of freedom than finite elements with strong imposition of symmetry.

Furthermore, the finite element exterior calculus, a rather abstract framework involving advanced mathematical tools, has been employed in the last two decades to derive new stable mixed finite element methods for linear elasticity, including strong symmetry and weakly imposed symmetry for the stresses (see, e.g., [7–10]). In particular, the first polynomial-based elements that are known to be stable for the symmetric stress-displacement formulation in 2D are those provided in [10]. The one of lowest order there involves 24 degrees of freedom per triangle to approximate the stress with piecewise cubic polynomials, whereas piecewise linear functions are used for the displacement. The 3D analogue of this element was proposed in [1], which considers piecewise quartic stresses with 162 degrees of freedom per tetrahedron, and piecewise linear displacements. In turn, new stable elements with a weakly imposed stress symmetry have been developed in [7,9,13]. The one with lowest polynomial degrees, known as the Arnold–Falk–Winther element of order 1, consists of piecewise linear approximations for the stress and piecewise constants functions for both the displacement and the rotation. From a different perspective, namely within the context of polytopal element methods, we may refer to [11], where a low-order virtual element yielding a symmetric approximation of the stress has been derived for two-dimensional elasticity problem. The analysis from [11] was extended in [12] to construct corresponding higher-order elements for the same model. An alternative to the aforementioned strong and weak symmetries, which can be understood as an approach in between these two concepts, was introduced in [23,24], where elements yielding continuous tangential components for the displacement, and continuous normal–normal component of the stress tensor, besides the symmetry of the latter, were defined.

On the other hand, augmented methods such as those proposed in [18,19,21] can provide finite elements that have even less degrees of freedom than those defined in [6,17,25], at the cost of increasing the fullness of the resulting system matrix and, sometimes, increasing also the regularity of other variables, such as displacements or velocities (and in particular, relaxing compatibility conditions between approximation spaces). Therefore, according to the above, here we propose and study an even weaker way to impose the symmetry of the stress, with the benefit of reducing the computational cost of augmented finite element methods since no further unknowns nor degrees of freedom are required. More precisely, we exploit the fact that, in many relevant applications, the symmetry of this tensor is given by its dependence on the strain or strain rate (the symmetric part of the displacement gradient or the velocity gradient tensors, respectively). In this way, we begin by describing this approach in the context of elastostatics taking [21] as a basis, to then reduce the computational cost of a method for the Boussinesq problem, taking this time [2] as a reference. On the one hand, we will see that some properties, such as bilinearity and boundedness of the involved operators, are a straightforward result of the analysis in the cited works; whereas the analysis of other features, such as ellipticity, will need to be redone (but using essentially the same tools). We will also see that this method does not require an additional regularity of other variables, it decreases the number of degrees of freedom of the system, and it still provides stress tensors that are asymptotically symmetric. It is also worthwhile to mention that, in the context of an augmented mixed method for the Navier–Stokes equations, the results from [14] provide a vorticity-free method resulting from a double integration by parts (as a way to impose mixed boundary conditions). Even if that scheme already uses a weaker imposition of symmetry (but not precisely the same as done in this paper), the authors in such work do not address the implications that this change could bring.

1.1 Outline

The rest of this work is organized as follows. First, we end this section by introducing some notation that will be used throughout this work, and then in Sect. 2 we present this weaker imposition of the symmetry of the stress tensor, and the resulting vorticity-free version of the continuous formulations presented in [2,21] for the elasticity and Boussinesq problems, respectively. Here, we focus on proving ellipticity of the bilinear forms, as this is the property that completely describes augmented methods. Next, in Sect. 3, we derive the corresponding Galerkin schemes for these formulations, to then in Sect. 4 present some numerical results that portray the main characteristics of the proposed augmented methods. Unless specified otherwise, the notation for spaces, finite dimensional subspaces, bilinear forms and functional are local to each problem.

1.2 Notation

Let us denote by $\Omega \subset \mathrm{R}^n$, $n \in \{2, 3\}$, a given bounded, simply connected domain with polyhedral boundary Γ, and denote by $\boldsymbol{\nu}$ the outward unit normal vector on Γ. Standard notation will be adopted for Lebesgue spaces $\mathrm{L}^p(\Omega)$ and Sobolev spaces $\mathrm{W}^{s,2}(\Omega) =: \mathrm{H}^s(\Omega)$ with norm $\|\cdot\|_{s,\Omega}$ and seminorm $|\cdot|_{s,\Omega}$. In particular, $\mathrm{H}^{1/2}(\Gamma)$

is the space of traces of functions in $\mathrm{H}^1(\Omega)$. By $\mathbf{M}$ and $\mathbb{M}$ we will denote the corresponding vectorial and tensorial counterparts of the generic scalar functional space M, and $\|\cdot\|$, with no subscripts, will stand for the natural norm of either an element or an operator in any product functional space. In turn, for any vector fields $\mathbf{v} = (v_i)_{i=\overline{1,n}}$ and $\mathbf{w} = (w_i)_{i=\overline{1,n}}$, we set the gradient, divergence and tensor product operators, as

$$\nabla \mathbf{v} := \left(\frac{\partial v_i}{\partial x_j} \right)_{i,j=\overline{1,n}}, \quad \mathrm{div}\, \mathbf{v} := \sum_{j=1}^{n} \frac{\partial v_j}{\partial x_j}, \quad \text{and} \quad \mathbf{v} \otimes \mathbf{w} := (v_i w_j)_{i,j=\overline{1,n}}.$$

In addition, for any tensor fields $\boldsymbol{\tau} = (\tau_{ij})_{i,j=\overline{1,n}}$ and $\boldsymbol{\zeta} = (\zeta_{ij})_{i,j=\overline{1,n}}$, we let $\mathbf{div}\, \boldsymbol{\tau}$ be the divergence operator div acting along the rows of $\boldsymbol{\tau}$, and define the transpose, the trace, the tensor inner product, and the deviatoric tensor, respectively, as

$$\boldsymbol{\tau}^{\mathrm{t}} := (\tau_{ji})_{i,j=\overline{1,n}}, \quad \mathrm{tr}(\boldsymbol{\tau}) := \sum_{i=1}^{n} \tau_{ii}, \quad \boldsymbol{\tau} : \boldsymbol{\zeta} := \sum_{i,j=1}^{n} \tau_{ij}\zeta_{ij}, \quad \text{and} \quad \boldsymbol{\tau}^{\mathrm{d}} := \boldsymbol{\tau} - \frac{1}{n}\mathrm{tr}(\boldsymbol{\tau})\mathbb{I},$$

where $\mathbb{I}$ stands for the identity tensor in $\mathbb{R} := \mathrm{R}^{n\times n}$. Furthermore, we recall that any tensor can be (uniquely) decomposed into its symmetric and skew-symmetric parts. In particular, for $\nabla \mathbf{v}$ this means that there exists tensors $\mathbf{e}(\mathbf{v})$ and $\boldsymbol{\omega}(\mathbf{v})$ such that

$$\nabla \mathbf{v} = \mathbf{e}(\mathbf{v}) + \boldsymbol{\omega}(\mathbf{v}) \quad \text{where} \quad \mathbf{e}(\mathbf{u}) := \frac{1}{2}\big(\nabla \mathbf{v} + (\nabla \mathbf{v})^{\mathrm{t}}\big) \quad \text{and} \quad \boldsymbol{\omega}(\mathbf{v}) := \frac{1}{2}\big(\nabla \mathbf{v} - (\nabla \mathbf{v})^{\mathrm{t}}\big). \tag{1.1}$$

We also recall that

$$\mathbb{H}(\mathbf{div}; \Omega) := \Big\{ \boldsymbol{\tau} \in \mathbb{L}^2(\Omega) \,:\, \mathbf{div}\, \boldsymbol{\tau} \in \mathbf{L}^2(\Omega) \Big\},$$

equipped with the usual norm

$$\| \boldsymbol{\tau} \|^2_{\mathbf{div};\Omega} := \| \boldsymbol{\tau} \|^2_{0,\Omega} + \| \mathbf{div}\, \boldsymbol{\tau} \|^2_{0,\Omega},$$

is a standard Hilbert space in the realm of mixed problems. In addition, there holds the decomposition $\mathbb{H}(\mathbf{div}; \Omega) = \mathbb{H}_0(\mathbf{div}; \Omega) \oplus \mathrm{R}\mathbb{I}$, where

$$\mathbb{H}_0(\mathbf{div}; \Omega) := \Big\{ \boldsymbol{\tau} \in \mathbb{H}(\mathbf{div}; \Omega) : \int_\Omega \mathrm{tr}(\boldsymbol{\tau}) = 0 \Big\}.$$

Finally, in what follows, $|\cdot|$ denotes the Euclidean norm in $\mathbf{R} := \mathrm{R}^n$, and we employ $\mathbf{0}$ to denote a generic null vector and use C, with or without subscripts, bars, tildes or hats, to mean generic positive constants independent of the discretization parameters, which may take different values at different places.

2 Continuous formulations with ultra-weak symmetry

We begin this section by recalling some results that will be used throughout this work to prove ellipticity of bilinear forms, since this is indeed the property that define admissible values for the stabilization parameters. Other properties such as boundedness of the bilinear forms are usually valid for just non-negative values of these parameters.

Lemma 2.1 *Let Ω be a bounded, simply connected domain with polyhedral boundary $\Gamma := \partial\Omega$. Then,*

(a) *there exists $c_1 > 0$ such that*

$$\begin{aligned} &\| \boldsymbol{\tau}^{\mathrm{d}} \|^2_{0,\Omega} + \| \mathbf{div}\, \boldsymbol{\tau} \|^2_{0,\Omega} \geq c_1 \| \boldsymbol{\tau}_0 \|^2_{0,\Omega} \\ &\forall\, \boldsymbol{\tau} = \boldsymbol{\tau}_0 + c\mathbb{I} \in \mathbb{H}(\mathbf{div};\Omega),\ \boldsymbol{\tau}_0 \in \mathbb{H}_0(\mathbf{div};\Omega),\ c \in \mathrm{R}, \end{aligned} \tag{2.1}$$

(b) *there exists $c_2 > 0$ such that*

$$\| \mathbf{e}(\mathbf{v}) \|^2_{0,\Omega} \geq c_2 |\, \mathbf{v} \,|^2_{1,\Omega} \quad \forall\, \mathbf{v} \in \mathbf{H}^1_0(\Omega), \tag{2.2}$$

with $c_2 = 0.5$ when $\Omega \subset \mathrm{R}^2$, and

(c) *there exists $c_3 > 0$ such that*

$$\| \mathbf{e}(\mathbf{v}) \|^2_{0,\Omega} + \| \mathbf{v} \|^2_{0,\Gamma} \geq c_3 \| \mathbf{v} \|^2_{1,\Omega} \quad \forall\, \mathbf{v} \in \mathbf{H}^1(\Omega). \tag{2.3}$$

Proof See [18, Lemma 2.1] for a), [22, Theorem 10.1] for b), [19, Lemma 3.1 and (3.9)] for c) when $\Omega \subset \mathrm{R}^2$, and [21, Lemma A.2] for c) when $\Omega \subset \mathrm{R}^3$. □

2.1 Linear elasticity

To introduce a weaker imposition of the symmetry of the stress tensor, let us consider an isotropic linear material occupying the three-dimensional region Ω in the context of elastostatics. Then, a simple model to describe this problem seeks a displacement $\mathbf{u}$ and a stress tensor $\boldsymbol{\sigma}$ such that

$$\boldsymbol{\sigma} = \mathscr{C}\mathbf{e}(\mathbf{u}) \quad \text{in } \Omega, \qquad -\mathbf{div}\,\boldsymbol{\sigma} = \mathbf{f} \quad \text{in } \Omega, \qquad \mathbf{u} = \mathbf{u}_D \quad \text{on } \Gamma, \tag{2.4}$$

where $\mathbf{f} \in \mathbf{L}^2(\Omega)$ is a volume force, $\mathbf{e}(\mathbf{u})$ is the strain tensor of small deformations [defined as in (1.1)], $\mathbf{u}_D \in \mathbf{H}^{1/2}(\Gamma)$ is a given Dirichlet datum for $\mathbf{u}$, and $\mathscr{C}$ is the fourth-order elasticity tensor, whose action, according to Hooke's Law, is given by

$$\mathscr{C}\boldsymbol{\zeta} := \lambda\, \mathrm{tr}(\boldsymbol{\zeta})\, \mathbb{I} + 2\,\mu\, \boldsymbol{\zeta} \quad \forall\, \boldsymbol{\zeta} \in \mathbb{L}^2(\Omega), \tag{2.5}$$

with λ, $\mu > 0$ being the corresponding Lamé constants. After a simple computation, it can be seen from this equation that the action of the compliance tensor is given by

$$\mathscr{C}^{-1}\boldsymbol{\zeta} = \frac{1}{2\mu}\boldsymbol{\zeta} - \frac{\lambda}{2\mu(2\mu+3\lambda)}\mathrm{tr}(\boldsymbol{\zeta})\mathbb{I} \quad \forall\, \boldsymbol{\zeta} \in \mathbb{L}^2(\Omega). \tag{2.6}$$

In this way, considering $\mathbf{e}(\mathbf{u}) = \nabla\mathbf{u} - \boldsymbol{\omega}(\mathbf{u})$ as in (1.1), the elasticity equations (2.4) can be rewritten as

$$\mathscr{C}^{-1}\boldsymbol{\sigma} = \nabla\mathbf{u} - \boldsymbol{\omega}(\mathbf{u}) \quad \text{in } \Omega, \qquad -\mathbf{div}\,\boldsymbol{\sigma} = \mathbf{f} \quad \text{in } \Omega, \qquad \mathbf{u} = \mathbf{u}_D \quad \text{on } \Gamma. \tag{2.7}$$

Then, a mixed formulation for this problem can be constructed by multiplying the first equation of (2.7) by a test function $\boldsymbol{\tau} \in \mathbb{H}(\mathbf{div}; \Omega)$ and integrating by parts, while the second equation is just tested with $\mathbf{v} \in \mathbf{L}^2(\Omega)$. The next step is to include in the formulation the symmetry of the Cauchy stress tensor with an additional term.

Differently from other works (e.g. [6,18,21]), we will not require additional unknowns, such as rotation or vorticity, to be computed. Moreover, we will not impose the symmetry of the stress tensor by considering it orthogonal (with respect to the standard L^2 inner product) to all skew-symmetric tensors in $\mathbb{L}^2(\Omega)$ (weak imposition), but rather to only those that can be written as the skew-symmetric part of a velocity gradient, that is

$$\int_\Omega \boldsymbol{\sigma} : \boldsymbol{\omega}(\mathbf{v}) = 0 \quad \forall\, \mathbf{v} \in \mathbf{H}^1(\Omega). \tag{2.8}$$

We also stress here that no further degrees of freedom either, but only those already provided by the velocity, are needed for (2.8). We refer to the addition of this term to the formulation as an "ultra-weak" imposition of the symmetry of $\boldsymbol{\sigma}$. In this way, at a first glance, the mixed formulation for (2.7) is given by: Find $(\boldsymbol{\sigma}, \mathbf{u}) \in \mathbb{H}(\mathbf{div}; \Omega) \times \mathbf{H}^1(\Omega)$ such that

$$\int_\Omega \mathscr{C}^{-1}\boldsymbol{\sigma} : \boldsymbol{\tau} + \int_\Omega \boldsymbol{\omega}(\mathbf{u}) : \boldsymbol{\tau} + \int_\Omega \mathbf{u} \cdot \mathbf{div}\,\boldsymbol{\tau} = \langle\, \boldsymbol{\tau}\boldsymbol{\nu}, \mathbf{u}_D \,\rangle_\Gamma \quad \forall\, \boldsymbol{\tau} \in \mathbb{H}(\mathbf{div}; \Omega), \tag{2.9a}$$

$$\int_\Omega \boldsymbol{\omega}(\mathbf{v}) : \boldsymbol{\sigma} + \int_\Omega \mathbf{v} \cdot \mathbf{div}\,\boldsymbol{\sigma} = -\int_\Omega \mathbf{f} \cdot \mathbf{v} \quad \forall\, \mathbf{v} \in \mathbf{H}^1(\Omega). \tag{2.9b}$$

The idea is to proceed with the analysis in the exact same terms as [21]. First, the stress tensor $\boldsymbol{\sigma}$ is decomposed as $\boldsymbol{\sigma} = \boldsymbol{\sigma}_0 + c\mathbb{I}$, with $\boldsymbol{\sigma}_0 \in \mathbb{H}_0(\mathbf{div}; \Omega)$ and $c \in \mathrm{R}$, which, taking $\boldsymbol{\tau} = \mathbb{I}$ in (2.9), yields the explicit knowledge of c in terms of $\mathbf{u}_D$. In this way, and after denoting the remaining unknown $\boldsymbol{\sigma}_0$ as simply $\boldsymbol{\sigma}$, we augment the formulation (2.9) with the following Galerkin-type terms:

$$\kappa_1 \int_\Omega \left\{\mathbf{e}(\mathbf{u}) - \mathscr{C}^{-1}\boldsymbol{\sigma}\right\} : \left\{\mathbf{e}(\mathbf{v}) + \mathscr{C}^{-1}\boldsymbol{\tau}\right\} = \kappa_1 \left(\frac{1}{3|\Omega|}\int_\Gamma \mathbf{u}_D \cdot \boldsymbol{\nu}\right) \int_\Omega \mathbb{I} : \left\{\mathbf{e}(\mathbf{v}) + \mathscr{C}^{-1}\boldsymbol{\tau}\right\},$$

$$\kappa_2 \int_\Omega \mathbf{div}\,\boldsymbol{\sigma} \cdot \mathbf{div}\,\boldsymbol{\tau} = -\kappa_2 \int_\Omega \mathbf{f} \cdot \mathbf{div}\,\boldsymbol{\tau},$$

$$\kappa_3 \int_\Gamma \mathbf{u} \cdot \mathbf{v} = \kappa_3 \int_\Gamma \mathbf{u}_D \cdot \mathbf{v}.$$

for all $(\boldsymbol{\tau}, \mathbf{v}) \in \mathbb{H}_0(\mathbf{div}; \Omega) \times \mathbf{H}^1(\Omega)$, with $\kappa_1, \kappa_2, \kappa_3 > 0$ positive stabilization parameters to be determined later on. Therefore, introducing the product space

$\mathcal{H} := \mathbb{H}_0(\mathbf{div};\Omega) \times \mathbf{H}^1(\Omega)$, the augmented mixed formulation of the elasticity problem (2.7) becomes: Find $(\boldsymbol{\sigma}, \mathbf{u}) \in \mathcal{H}$ such that

$$\mathbf{A}((\boldsymbol{\sigma}, \mathbf{u}), (\boldsymbol{\tau}, \mathbf{v})) = \mathbf{F}(\boldsymbol{\tau}, \mathbf{v}) \quad \forall\, (\boldsymbol{\tau}, \mathbf{v}) \in \mathcal{H}, \tag{2.10}$$

where the form $\mathbf{A} : \mathcal{H} \times \mathcal{H} \to \mathrm{R}$ and the functional $\mathbf{F} : \mathcal{H} \to \mathrm{R}$ are given by

$$\begin{aligned}\mathbf{A}((\boldsymbol{\sigma}, \mathbf{u}), (\boldsymbol{\tau}, \mathbf{v})) := &\int_\Omega \mathscr{C}^{-1}\boldsymbol{\sigma} : \boldsymbol{\tau} + \int_\Omega \boldsymbol{\omega}(\mathbf{u}) : \boldsymbol{\tau} + \int_\Omega \mathbf{u} \cdot \mathbf{div}\, \boldsymbol{\tau} \\ &- \int_\Omega \boldsymbol{\omega}(\mathbf{v}) : \boldsymbol{\sigma} - \int_\Omega \mathbf{v} \cdot \mathbf{div}\, \boldsymbol{\sigma} \\ &+\kappa_1 \int_\Omega \left\{\mathbf{e}(\mathbf{u}) - \mathscr{C}^{-1}\boldsymbol{\sigma}\right\} : \left\{\mathbf{e}(\mathbf{v}) + \mathscr{C}^{-1}\boldsymbol{\tau}\right\} \\ &+\kappa_2 \int_\Omega \mathbf{div}\, \boldsymbol{\sigma} \cdot \mathbf{div}\, \boldsymbol{\tau} + \kappa_3 \int_\Gamma \mathbf{u} \cdot \mathbf{v}\,,\end{aligned} \tag{2.11}$$

and

$$\begin{aligned}\mathbf{F}(\boldsymbol{\tau}, \mathbf{v}) = &\int_\Omega \mathbf{f} \cdot \left\{\mathbf{v} - \kappa_2 \mathbf{div}\, \boldsymbol{\tau}\right\} + \kappa_1 \left(\frac{1}{3|\Omega|} \int_\Gamma \mathbf{u}_D \cdot \boldsymbol{\nu}\right) \int_\Gamma \mathbf{v} \cdot \boldsymbol{\nu} \\ &+\langle\, \boldsymbol{\tau}\boldsymbol{\nu}, \mathbf{u}_D \,\rangle_\Gamma + \kappa_3 \int_\Gamma \mathbf{u}_D \cdot \mathbf{v},\end{aligned} \tag{2.12}$$

for all $(\boldsymbol{\sigma}, \mathbf{u}), (\boldsymbol{\tau}, \mathbf{v}) \in \mathcal{H}$. In what follows we see that the incorporation of (2.8) and the augmentation procedure play key roles in this formulation. More precisely, we now define the norm in $\mathcal{H}$ as

$$\|\, (\boldsymbol{\tau}, \mathbf{v}) \,\|_{\mathcal{H}} := \left\{ \|\, \boldsymbol{\tau} \,\|^2_{\mathbf{div},\Omega} + \|\, \mathbf{v} \,\|^2_{1,\Omega} \right\}^{1/2},$$

and establish the ellipticity of $\mathbf{A}$ by considering suitable ranges for the stabilization parameters.

Lemma 2.2 *Assume that $\kappa_1 \in (0, 2\mu)$ and $\kappa_2, \kappa_3 \in (0, \infty)$. Then, there exists $\alpha(\Omega) > 0$ independent of λ, such that*

$$\mathbf{A}((\boldsymbol{\tau}, \mathbf{v}), (\boldsymbol{\tau}, \mathbf{v})) \geq \alpha(\Omega) \|\, (\boldsymbol{\tau}, \mathbf{v}) \,\|^2_{\mathcal{H}} \quad \forall\, (\boldsymbol{\tau}, \mathbf{v}) \in \mathcal{H}. \tag{2.13}$$

Proof First, we rewrite the first term that defines $\mathbf{A}$ [cf. (2.11)] as

$$\int_\Omega \mathscr{C}^{-1}\boldsymbol{\sigma} : \boldsymbol{\tau} = \frac{1}{2\mu} \int_\Omega \boldsymbol{\sigma}^{\mathrm{d}} : \boldsymbol{\tau}^{\mathrm{d}} + \frac{1}{3(2\mu + 3\lambda)} \int_\Omega \mathrm{tr}(\boldsymbol{\sigma})\, \mathrm{tr}(\boldsymbol{\tau}).$$

Then, for any $(\boldsymbol{\tau}, \mathbf{v}) \in \mathcal{H}$, we see that

$$\begin{aligned}
&\mathbf{A}((\boldsymbol{\tau}, \mathbf{v}), (\boldsymbol{\tau}, \mathbf{v})) \\
&\quad = \int_\Omega \mathscr{C}^{-1}\boldsymbol{\tau} : \boldsymbol{\tau} - \kappa_1 \left\| \mathscr{C}^{-1}\boldsymbol{\tau} \right\|_{0,\Omega}^2 + \kappa_1 \| \mathbf{e}(\mathbf{v}) \|_{0,\Omega}^2 + \kappa_2 \| \mathbf{div}\, \boldsymbol{\tau} \|_{0,\Omega}^2 + \kappa_3 \| \mathbf{v} \|_{0,\Gamma}^2 \\
&\quad = \frac{1}{2\mu}\left(1 - \frac{\kappa_1}{2\mu}\right) \| \boldsymbol{\tau}^{\mathrm{d}} \|_{0,\Omega}^2 + \frac{1}{3(2\mu + 3\lambda)}\left(1 - \frac{\kappa_1}{2\mu + 3\lambda}\right) \| \mathrm{tr}(\boldsymbol{\tau}) \|_{0,\Omega}^2 \\
&\qquad + \kappa_1 \| \mathbf{e}(\mathbf{v}) \|_{0,\Omega}^2 + \kappa_2 \| \mathbf{div}\, \boldsymbol{\tau} \|_{0,\Omega}^2 + \kappa_3 \| \mathbf{v} \|_{0,\Gamma}^2. \qquad (2.14)
\end{aligned}$$

Notice that, if $\kappa_1 < 2\mu$, then not only $1 - \frac{\kappa_1}{2\mu} > 0$ but also $1 - \frac{\kappa_1}{2\mu + 3\lambda} > 0$. Therefore, discarding the term with $\| \mathrm{tr}(\boldsymbol{\tau}) \|_{0,\Omega}^2$, and using Lemma 2.1, there holds for any $(\boldsymbol{\tau}, \mathbf{v}) \in \mathcal{H}$ that

$$\mathbf{A}((\boldsymbol{\tau}, \mathbf{v}), (\boldsymbol{\tau}, \mathbf{v})) \geq \alpha_1 c_1 \| \boldsymbol{\tau} \|_{0,\Omega}^2 + \frac{\kappa_2}{2} \| \mathbf{div}\, \boldsymbol{\tau} \|_{0,\Omega}^2 + \alpha_2 c_3 \| \mathbf{v} \|_{1,\Omega}^2,$$

where

$$\alpha_1 := \min\left\{ \frac{1}{2\mu}\left(1 - \frac{\kappa_1}{2\mu}\right), \frac{\kappa_2}{2} \right\} \quad \text{and} \quad \alpha_2 := \min\{\kappa_1, \kappa_3\}.$$

In this way, denoting by

$$\alpha_3 := \min\left\{ \alpha_1 c_1, \frac{\kappa_2}{2} \right\}$$

there exists $\alpha(\Omega) := \min\{\alpha_3, \alpha_2 c_3\}$, clearly independent of λ, such that (2.13) holds. □

At this point we remark that, thanks to the ultra-weak imposition (2.8) of the symmetry of $\boldsymbol{\sigma}$ and its consequent incorporation into the formulation, the second and fourth terms on the right hand side of (2.11) cancel out when $(\boldsymbol{\sigma}, \mathbf{u}) = (\boldsymbol{\tau}, \mathbf{v})$, which is reflected in the identity (2.14), thus allowing to easily prove the ellipticity of $\mathbf{A}$. Otherwise, if (2.8) is not included, the expression that arises from the aforementioned second term, namely $\int_\Omega \boldsymbol{\omega}(\mathbf{v}) : \boldsymbol{\tau}$, would stop us of proving that property, unless certain restrictions involving the Lamé constant μ, the parameters κ_1 and κ_3, and the unknown constant c_3 (cf. (2.3), Lemma 2.1), are imposed. In turn, as it will be observed later on in Sect. 3.1, the ellipticity of $\mathbf{A}$ certainly yields the corresponding Céa estimate, which is actually what, together with the symmetry of $\boldsymbol{\sigma}$, will imply the asymptotic symmetry of the discrete stresses.

For computational purposes, and based on the proof of the previous Lemma, we can use the following stabilization parameters to make α as large as possible: $\kappa_1 = \mu$, $\kappa_2 = \frac{1}{2\mu}$ and $\kappa_3 = \kappa_1 = \mu$. Thus, the Lax–Milgram theorem (see, e.g., [20, Theorem 1.1]) provides the well-posedness result for (2.10) in similar terms as [21, Theorem 3.2].

Theorem 2.3 *Under the assumptions of Lemma 2.2, there exists a unique* $(\boldsymbol{\sigma}, \mathbf{u}) \in \mathcal{H}$ *solution to the weak formulation* (2.10)*. Moreover, there exists* $C > 0$*, independent of* λ*, such that*

$$\| (\boldsymbol{\sigma}, \mathbf{u}) \|_{\mathcal{H}} \leq \frac{\| \mathbf{F} \|}{\alpha(\Omega)} \leq C \Big\{ \| \mathbf{f} \|_{0,\Omega} + \| \mathbf{u}_D \|_{1/2,\Gamma} \Big\}. \tag{2.15}$$

Proof We remark that $\| \mathbf{e}(\mathbf{v}) \|_{0,\Omega}, \| \boldsymbol{\omega}(\mathbf{v}) \|_{0,\Omega} \leq \| \mathbf{v} \|_{1,\Omega}$ for any $\mathbf{v} \in \mathbf{H}^1(\Omega)$, and therefore, it is straightforward from [21, Theorem 3.1] that $\mathbf{A}$ is a bilinear and bounded form in $\mathcal{H} \times \mathcal{H}$, since it is a reduced version of the one considered there as no vorticity-related terms have been added. On the other hand, it is clear that the term in brackets at the right hand side of (2.15) is nothing but a bound for $\| \mathbf{F} \|$. Therefore, Lemma 2.2 and the foregoing arguments satisfy the hypotheses of the Lax–Milgram theorem, thus getting existence and uniqueness for (2.10). □

2.2 Boussinesq problem with nonconstant physical properties

Any reduction in the computational cost of a numerical method is valuable, but perhaps it is more desirable when a high number of variables and degrees of freedom is inevitable, as in the case of fully-mixed methods for coupled problems in three dimensions. Indeed, we now consider the flow of a non-isothermal, incompressible, Newtonian fluid with varying viscosity within a region Ω. Then, a model for this phenomenon is given by a generalized version of the Boussinesq equations, that when considered in the form [2], and neglecting the definition of the vorticity, seeks a rate of strain $\mathbf{t}$, a pseudostress $\boldsymbol{\sigma}$, a velocity $\mathbf{u}$, a temperature gradient (o diffusive heat flux) $\boldsymbol{\zeta}$, a total heat flux $\mathbf{p}$, and a temperature φ such that

$$\begin{aligned}
&-\nabla \mathbf{u} + \mathbf{t} + \boldsymbol{\omega}(\mathbf{u}) = \mathbf{0} \quad \text{in } \Omega, \quad \mu(\varphi)\mathbf{t} - (\mathbf{u} \otimes \mathbf{u})^{\mathrm{d}} - \boldsymbol{\sigma}^{\mathrm{d}} = \mathbf{0} \quad \text{in } \Omega, \\
&-\mathbf{div}\, \boldsymbol{\sigma} - \varphi \mathbf{g} = \mathbf{f}^{\mathrm{m}} \quad \text{in } \Omega, \quad \mathbf{u} = \mathbf{0} \quad \text{on } \Gamma, \quad \int_{\Omega} \mathrm{tr}(\boldsymbol{\sigma} + \mathbf{u} \otimes \mathbf{u}) = 0, \\
&-\nabla \varphi + \boldsymbol{\zeta} = \mathbf{0} \quad \text{in } \Omega, \quad \mathbf{p} = k(\varphi)\boldsymbol{\zeta} - \varphi \mathbf{u} \quad \text{in } \Omega, \\
&-\mathrm{div}\, \mathbf{p} = f^{\mathrm{e}} \quad \text{in } \Omega, \quad \varphi = \varphi_D \quad \text{on } \Gamma_D, \quad \mathbf{p} \cdot \boldsymbol{\nu} = 0 \quad \text{on } \Gamma_N,
\end{aligned} \tag{2.16}$$

where the boundary $\partial\Omega =: \Gamma$ has been split as $\Gamma = \Gamma_D \cup \Gamma_N$ with $\Gamma_D \cap \Gamma_N = \emptyset$, $-\mathbf{g} \in \mathbf{L}^{\infty}(\Omega)$ is a body force, $\mathbf{f}^{\mathrm{m}} \in \mathbf{L}^2(\Omega)$ and $f^{\mathrm{e}} \in \mathrm{L}^2(\Omega)$ are source terms, and $\varphi_D \in \mathrm{H}^{1/2}(\Gamma_D)$ is a prescribed temperature on part of the boundary. Furthermore, $\mu, k : \mathrm{R} \to \mathrm{R}^+$ are temperature-dependent viscosity and thermal conductivity functions, respectively, which are assumed to be bounded and Lipschitz continuous, that is, there exists $\mu_2 \geq \mu_1 > 0$, $L_\mu > 0$, $k_2 \geq k_1 > 0$, $L_k > 0$ such that for any $s, t \in \mathrm{R}$

$$\mu_1 \leq \mu(t) \leq \mu_2, \quad |\mu(s) - \mu(t)| \leq L_\mu |s - t| \tag{2.17}$$

and

$$k_1 \leq k(t) \leq k_2, \quad |k(s) - k(t)| \leq L_k |s - t|. \tag{2.18}$$

On the one hand, recalling that $\mathbf{t} = \mathbf{e}(\mathbf{u})$ is a symmetric, null-trace tensor (the fluid is incompressible), we take into consideration the space:

$$\mathbb{L}^2_{\mathtt{tr}}(\Omega) := \Big\{ \mathbf{s} \in \mathbb{L}^2(\Omega) : \mathbf{s} = \mathbf{s}^{\mathtt{t}} \text{ and } \mathrm{tr}(\mathbf{s}) = 0 \Big\}.$$

On the other hand, the Neumann condition for the total heat flux leads us to consider for this variable the space:

$$\mathbf{H}_{\mathrm{N}}(\mathrm{div};\Omega) := \Big\{ \mathbf{q} \in \mathbf{H}(\mathrm{div};\Omega) : \quad \mathbf{q}\cdot\boldsymbol{\nu} = 0 \quad \text{on } \Gamma_N \}.$$

In this way, integrating by parts the first and sixth equation of (2.16) and properly testing the remaining equations (see [2, Section 3.1] for more details), a fully-mixed weak formulation for (2.16) with ultra-weak symmetry is given by: Find $(\mathbf{t}, \boldsymbol{\sigma}, \mathbf{u}, \boldsymbol{\zeta}, \mathbf{p}, \varphi) \in \mathbb{L}^2_{\mathtt{tr}}(\Omega) \times \mathbb{H}_0(\mathbf{div};\Omega) \times \mathbf{H}^1_0(\Omega) \times \mathbf{L}^2(\Omega) \times \mathbf{H}_{\mathrm{N}}(\mathrm{div};\Omega) \times \mathrm{H}^1(\Omega)$ such that

$$\begin{aligned}
\int_\Omega \mu(\varphi)\mathbf{t} : \mathbf{s} - \int_\Omega (\mathbf{u}\otimes\mathbf{u})^{\mathtt{d}} : \mathbf{s} - \int_\Omega \boldsymbol{\sigma}^{\mathtt{d}} : \mathbf{s} &= 0 && \forall\, \mathbf{s} \in \mathbb{L}^2_{\mathtt{tr}}(\Omega),\\
\int_\Omega \mathbf{t} : \boldsymbol{\tau}^{\mathtt{d}} + \int_\Omega \boldsymbol{\omega}(\mathbf{u}) : \boldsymbol{\tau} + \int_\Omega \mathbf{u}\cdot\mathbf{div}\,\boldsymbol{\tau} &= 0 && \forall\, \boldsymbol{\tau} \in \mathbb{H}_0(\mathbf{div};\Omega),\\
-\int_\Omega \boldsymbol{\omega}(\mathbf{v}) : \boldsymbol{\sigma} - \int_\Omega \mathbf{v}\cdot\mathbf{div}\,\boldsymbol{\sigma} &= \int_\Omega \Big\{\varphi\mathbf{g} + \mathbf{f}^{\mathrm{m}}\Big\}\cdot\mathbf{v} && \forall\, \mathbf{v} \in \mathbf{H}^1_0(\Omega),\\
\int_\Omega k(\varphi)\,\boldsymbol{\zeta}\cdot\boldsymbol{\chi} - \int_\Omega \varphi\mathbf{u}\cdot\boldsymbol{\chi} - \int_\Omega \mathbf{p}\cdot\boldsymbol{\chi} &= 0 && \forall\, \boldsymbol{\chi} \in \mathbf{L}^2(\Omega),\\
\int_\Omega \boldsymbol{\zeta}\cdot\mathbf{q} + \int_\Omega \varphi\,\mathrm{div}\,\mathbf{q} &= \langle\, \mathbf{q}\cdot\boldsymbol{\nu}, \varphi_D \,\rangle_{\Gamma_D} && \forall\, \mathbf{q} \in \mathbf{H}_{\mathrm{N}}(\mathrm{div};\Omega),\\
-\int_\Omega \psi\,\mathrm{div}\,\mathbf{p} &= \int_\Omega f^{\mathrm{e}}\,\psi && \forall\, \psi \in \mathrm{H}^1(\Omega).
\end{aligned} \tag{2.19}$$

Notice that the ultra-weak imposition of the symmetry of the pseudostress tensor has been included as the first term in the third equation of (2.19). Then, we proceed to augment this formulation with the following terms:

$$\begin{aligned}
\kappa_1 \int_\Omega \Big\{\boldsymbol{\sigma}^{\mathtt{d}} + (\mathbf{u}\otimes\mathbf{u})^{\mathtt{d}} - \mu(\varphi)\mathbf{t}\Big\} : \boldsymbol{\tau}^{\mathtt{d}} &= 0 && \forall\, \boldsymbol{\tau} \in \mathbb{H}_0(\mathbf{div};\Omega),\\
\kappa_2 \int_\Omega \mathbf{div}\,\boldsymbol{\sigma}\cdot\mathbf{div}\,\boldsymbol{\tau} &= -\kappa_2 \int_\Omega \Big\{\varphi\mathbf{g} + \mathbf{f}^{\mathrm{m}}\Big\}\cdot\mathbf{div}\,\boldsymbol{\tau} && \forall\, \boldsymbol{\tau} \in \mathbb{H}_0(\mathbf{div};\Omega),\\
\kappa_3 \int_\Omega \Big\{\mathbf{e}(\mathbf{u}) - \mathbf{t}\Big\} : \mathbf{e}(\mathbf{v}) &= 0 && \forall\, \mathbf{v} \in \mathbf{H}^1_0(\Omega),\\
\kappa_4 \int_\Omega \Big\{\mathbf{p} + \varphi\mathbf{u} - k(\varphi)\boldsymbol{\zeta}\Big\}\cdot\mathbf{q} &= 0 && \forall\, \mathbf{q} \in \mathbf{H}_{\mathrm{N}}(\mathrm{div};\Omega),\\
\kappa_5 \int_\Omega \mathrm{div}\,\mathbf{p}\,\mathrm{div}\,\mathbf{q} &= -\kappa_5 \int_\Omega f^{\mathrm{e}}\,\mathrm{div}\,\mathbf{q} && \forall \mathbf{q} \in \mathbf{H}_{\mathrm{N}}(\mathrm{div};\Omega),
\end{aligned}$$

$$\kappa_6 \int_\Omega \Big\{\nabla\varphi - \boldsymbol{\zeta}\Big\}\cdot\nabla\psi = 0 \qquad \forall\ \psi \in \mathrm{H}^1(\Omega),$$
$$\kappa_7 \int_{\Gamma_D} \varphi\,\psi = \kappa_7 \int_{\Gamma_D} \varphi_D\,\psi \qquad \forall\ \psi \in \mathrm{H}^1(\Omega)\,.$$

Next, denoting by

$$\mathcal{H} := \mathbb{L}^2_{\mathtt{tr}}(\Omega)\times\mathbb{H}_0(\mathbf{div};\Omega)\times\mathbf{H}^1_0(\Omega), \quad \mathcal{Q} := \mathbf{L}^2(\Omega)\times\mathbf{H}_{\mathrm{N}}(\mathrm{div};\Omega)\times\mathrm{H}^1(\Omega),$$
$$\vec{\mathbf{t}} := (\mathbf{t},\boldsymbol{\sigma},\mathbf{u}), \quad \vec{\mathbf{s}} := (\mathbf{s},\boldsymbol{\tau},\mathbf{v}), \quad \vec{\boldsymbol{\zeta}} := (\boldsymbol{\zeta},\mathbf{p},\varphi), \quad \vec{\boldsymbol{\chi}} := (\boldsymbol{\chi},\mathbf{q},\psi),$$

the augmented fully-mixed formulation of (2.16) is: Find $(\vec{\mathbf{t}},\vec{\boldsymbol{\zeta}})\in\mathcal{H}\times\mathcal{Q}$ such that

$$\begin{aligned} \mathbf{A}_\varphi(\vec{\mathbf{t}},\vec{\mathbf{s}}) + \mathbf{B}_{\mathbf{u}}(\vec{\mathbf{t}},\vec{\mathbf{s}}) &= F_\varphi(\vec{\mathbf{s}}) + F_{\mathrm{m}}(\vec{\mathbf{s}}) \qquad \forall\ \vec{\mathbf{s}}\in\mathcal{H},\\ \mathbf{C}_\varphi(\vec{\boldsymbol{\zeta}},\vec{\boldsymbol{\chi}}) + \mathbf{D}_{\mathbf{u}}(\vec{\boldsymbol{\zeta}},\vec{\boldsymbol{\chi}}) &= G_D(\vec{\boldsymbol{\chi}}) + G_{\mathrm{e}}(\vec{\boldsymbol{\chi}}) \qquad \forall\ \vec{\boldsymbol{\chi}}\in\mathcal{Q}, \end{aligned} \tag{2.20}$$

where, given $(\mathbf{w},\phi)\in\mathbf{H}^1(\Omega)\times\mathrm{H}^1(\Omega)$, the bilinear forms $\mathbf{A}_\phi$, $\mathbf{B}_{\mathbf{w}}$, $\mathbf{C}_\phi$, $\mathbf{D}_{\mathbf{w}}$ and the linear functionals F_ϕ, F_{m}, G_D and G_{e} are defined as:

$$\begin{aligned} \mathbf{A}_\phi(\vec{\mathbf{t}},\vec{\mathbf{s}}) \;=\; & \int_\Omega \mu(\phi)\mathbf{t} : \big\{\mathbf{s} - \kappa_1\boldsymbol{\tau}^{\mathtt{d}}\big\} + \int_\Omega \mathbf{t} : \big\{\boldsymbol{\tau}^{\mathtt{d}} - \kappa_3\mathbf{e}(\mathbf{v})\big\} - \int_\Omega \boldsymbol{\sigma}^{\mathtt{d}} : \big\{\mathbf{s} - \kappa_1\boldsymbol{\tau}^{\mathtt{d}}\big\}\\ & + \int_\Omega \mathbf{u}\cdot\mathbf{div}\,\boldsymbol{\tau} + \int_\omega \boldsymbol{\omega}(\mathbf{u}) : \boldsymbol{\tau} - \int_\Omega \mathbf{v}\cdot\mathbf{div}\,\boldsymbol{\sigma} - \int_\Omega \boldsymbol{\omega}(\mathbf{v}) : \boldsymbol{\sigma}\\ & + \kappa_2\int_\Omega \mathbf{div}\,\boldsymbol{\sigma}\cdot\mathbf{div}\,\boldsymbol{\tau} + \kappa_3\int_\Omega \mathbf{e}(\mathbf{u}) : \mathbf{e}(\mathbf{v}), \end{aligned} \tag{2.21}$$

$$\mathbf{B}_{\mathbf{w}}(\vec{\mathbf{t}},\vec{\mathbf{s}}) := -\int_\Omega (\mathbf{u}\otimes\mathbf{w})^{\mathtt{d}} : \big\{\mathbf{s} - \kappa_1\boldsymbol{\tau}^{\mathtt{d}}\big\}, \tag{2.22}$$

for all $\vec{\mathbf{t}},\vec{\mathbf{s}}\in\mathcal{H}$;

$$\begin{aligned} \mathbf{C}_\phi(\vec{\boldsymbol{\zeta}},\vec{\boldsymbol{\chi}}) := & \int_\Omega k(\phi)\boldsymbol{\zeta}\cdot\big\{\boldsymbol{\chi} - \kappa_4\mathbf{q}\big\} + \int_\Omega \boldsymbol{\zeta}\cdot\big\{\mathbf{q} - \kappa_6\nabla\psi\big\} - \int_\Omega \mathbf{p}\cdot\big\{\boldsymbol{\chi} - \kappa_4\mathbf{q}\big\}\\ & + \int_\Omega \varphi\,\mathrm{div}\,\mathbf{q} - \int_\Omega \psi\,\mathrm{div}\,\mathbf{p} + \kappa_5\int_\Omega \mathrm{div}\,\mathbf{p}\,\mathrm{div}\,\mathbf{q} + \kappa_6\int_\Omega \nabla\varphi\cdot\nabla\psi + \kappa_7\int_{\Gamma_D}\varphi\,\psi, \end{aligned} \tag{2.23}$$

$$\mathbf{D}_{\mathbf{w}}(\vec{\boldsymbol{\zeta}},\vec{\boldsymbol{\chi}}) := -\int_\Omega \varphi\mathbf{w}\cdot\big\{\boldsymbol{\chi} - \kappa_4\mathbf{q}\big\}, \tag{2.24}$$

for all $\vec{\boldsymbol{\zeta}},\vec{\boldsymbol{\chi}}\in\mathcal{Q}$;

$$F_\phi(\vec{\mathbf{s}}) := \int_\Omega \phi\mathbf{g}\cdot\big\{\mathbf{v} - \kappa_2\mathbf{div}\,\boldsymbol{\tau}\big\}, \tag{2.25}$$

$$F_{\mathrm{m}}(\vec{\mathbf{s}}) := \int_\Omega \mathbf{f}^{\mathrm{m}}\cdot\big\{\mathbf{v} - \kappa_2\mathbf{div}\,\boldsymbol{\tau}\big\}, \tag{2.26}$$

for all $\vec{\mathbf{s}} \in \mathcal{H}$;

$$G_D(\vec{\boldsymbol{\chi}}) := \langle \mathbf{q} \cdot \boldsymbol{\nu}, \varphi_D \rangle_{\Gamma_D} + \kappa_7 \int_{\Gamma_D} \varphi_D \, \psi, \tag{2.27}$$

$$G_{\mathrm{e}}(\vec{\boldsymbol{\chi}}) := \int_{\Omega} f^{\mathrm{e}} \left\{ \psi - \kappa_5 \mathrm{div}\, \mathbf{q} \right\}, \tag{2.28}$$

for all $\vec{\boldsymbol{\chi}} \in \mathcal{Q}$. Now, we decouple (2.20) following [2, Section 3.2] (see, also [5,15,16]), and rewrite it as a fixed-point problem. Indeed, we denote $\mathbf{H} := \mathbf{H}^1_0(\Omega) \times \mathrm{H}^1(\Omega)$ and consider first the operator $\mathbf{M} : \mathbf{H} \to \mathcal{H}$ defined as

$$\mathbf{M}(\mathbf{w}, \phi) = \Big(\mathbf{M}_1(\mathbf{w}, \phi), \mathbf{M}_2(\mathbf{w}, \phi), \mathbf{M}_3(\mathbf{w}, \phi) \Big) := \vec{\mathbf{t}},$$

where $\vec{\mathbf{t}} \in \mathcal{H}$ is the solution to:

$$\mathbf{A}_\phi(\vec{\mathbf{t}}, \vec{\mathbf{s}}) + \mathbf{B}_{\mathbf{w}}(\vec{\mathbf{t}}, \vec{\mathbf{s}}) = F_\phi(\vec{\mathbf{s}}) + F_{\mathrm{m}}(\vec{\mathbf{s}}) \quad \forall\, \vec{\mathbf{s}} \in \mathcal{H}. \tag{2.29}$$

Then, consider the operator $\mathbf{E} : \mathbf{H} \to \mathcal{Q}$ defined as

$$\mathbf{E}(\mathbf{w}, \phi) = \Big(\mathbf{E}_1(\mathbf{w}, \phi), \mathbf{E}_2(\mathbf{w}, \phi), \mathbf{E}_3(\mathbf{w}, \phi) \Big) := \vec{\boldsymbol{\zeta}},$$

where $\vec{\boldsymbol{\zeta}} \in \mathcal{Q}$ is now the solution to:

$$\mathbf{C}_\phi(\vec{\boldsymbol{\zeta}}, \vec{\boldsymbol{\chi}}) + \mathbf{D}_{\mathbf{w}}(\vec{\boldsymbol{\zeta}}, \vec{\boldsymbol{\chi}}) = G_D(\vec{\boldsymbol{\chi}}) + G_{\mathrm{e}}(\vec{\boldsymbol{\chi}}) \quad \forall\, \vec{\boldsymbol{\chi}} \in \mathcal{Q}. \tag{2.30}$$

Consequently, we can define the operator $\mathbf{T} : \mathbf{H} \to \mathbf{H}$ as

$$\mathbf{T}(\mathbf{w}, \phi) := \Big(\mathbf{M}_3(\mathbf{w}, \phi), \mathbf{E}_3(\mathbf{M}_3(\mathbf{w}, \phi), \phi) \Big), \tag{2.31}$$

and transform (2.20) into the problem: Find $(\mathbf{u}, \varphi) \in \mathbf{H}$ such that

$$\mathbf{T}(\mathbf{u}, \varphi) = (\mathbf{u}, \varphi). \tag{2.32}$$

Again, the similarity of $\mathbf{A}_\phi + \mathbf{B}_{\mathbf{w}}$ with respect to the one defined in [2] leads us to only analyze its ellipticity to conclude that (2.32) is a well-posed problem. In this regard, and similarly as remarked right after the proof of Lemma 2.2, we notice here in advance that, besides the inclusion of the augmented terms, the incorporation of the expression $\int_\Omega \boldsymbol{\omega}(\mathbf{v}) : \boldsymbol{\sigma}$ in the third equation of (2.19), and then in the definition of the form $\mathbf{A}_\phi$ [cf. (2.21)], is crucial as well for the aforementioned ellipticity, as it is shown next.

Lemma 2.4 *Assume that for* $\delta_1 \in \left(0, \frac{2}{\mu_2}\right)$ *and* $\delta_2 \in (0, 2)$ *we choose*

$$\kappa_1 \in \left(0, \frac{2\delta_1\mu_1}{\mu_2}\right), \quad \kappa_2 \in (0, \infty) \quad \textit{and} \quad \kappa_3 \in \left(0, 2\delta_2 \left(\mu_1 - \frac{\kappa_1\mu_2}{2\delta_1}\right)\right).$$

Then, there exists $r_1 > 0$ such that for each $r \in (0, r_1)$, the bilinear form $\mathbf{A}_\phi + \mathbf{B}_\mathbf{w}$ is elliptic in $\mathcal{H}$ for each $(\mathbf{w}, \phi) \in \mathbf{H}$ such that $\| \mathbf{w} \|_{1,\Omega} \leq r$. More precisely, there exists $\alpha(\Omega) > 0$ such that

$$(\mathbf{A}_\phi + \mathbf{B}_\mathbf{w})(\vec{\mathbf{s}}, \vec{\mathbf{s}}) \geq \frac{\alpha(\Omega)}{2} \| \vec{\mathbf{s}} \|^2 \quad \forall\, \vec{\mathbf{s}} \in \mathcal{H}. \tag{2.33}$$

Proof Let $(\mathbf{w}, \phi) \in \mathbf{H}$ and $\vec{\mathbf{s}} \in \mathcal{H}$. Then, noting from (2.21) that when $\vec{\mathbf{t}} = \vec{\mathbf{s}}$ the corresponding fifth and seventh terms on the right hand side cancel out, we deduce that for $\mathbf{A}_\phi$ there holds

$$\begin{aligned}\mathbf{A}_\phi(\vec{\mathbf{s}}, \vec{\mathbf{s}}) = \int_\Omega \mu(\phi)\mathbf{s} : \mathbf{s} - \kappa_1 \int_\Omega \mu(\phi)\mathbf{s} : \boldsymbol{\tau}^{\mathrm{d}} - \kappa_3 \int_\Omega \mathbf{s} : \mathbf{e}(\mathbf{v}) \\ + \kappa_1 \| \boldsymbol{\tau}^{\mathrm{d}} \|^2_{0,\Omega} + \kappa_2 \| \mathbf{div}\, \boldsymbol{\tau} \|^2_{0,\Omega} + \kappa_3 \| \mathbf{e}(\mathbf{v}) \|^2_{0,\Omega}.\end{aligned}$$

Then, using the bounds of the viscosity function (2.17), the Cauchy-Schwarz and Young inequalities and Lemma 2.1, we obtain for any $\delta_1, \delta_2 > 0$ that

$$\begin{aligned}\mathbf{A}_\phi(\vec{\mathbf{s}}, \vec{\mathbf{s}}) \geq \left(\mu_1 - \frac{\kappa_1\mu_2}{2\delta_1} - \frac{\kappa_3}{2\delta_2}\right) \| \mathbf{s} \|^2_{0,\Omega} + \kappa_1 \left(1 - \frac{\mu_2\delta_1}{2}\right) \| \boldsymbol{\tau}^{\mathrm{d}} \|^2_{0,\Omega} \\ + \kappa_2 \| \mathbf{div}\, \boldsymbol{\tau} \|^2_{0,\Omega} + \kappa_3 \left(1 - \frac{\delta_2}{2}\right) \| \mathbf{e}(\mathbf{v}) \|^2_{0,\Omega},\end{aligned}$$

and therefore, defining

$$\begin{aligned}&\alpha_1 := \mu_1 - \frac{\kappa_1\mu_2}{2\delta_1} - \frac{\kappa_3}{2\delta_2}, \quad \alpha_2 := \min\left\{\kappa_1\left(1 - \frac{\mu_2\delta_1}{2}\right), \frac{\kappa_2}{2}\right\}, \\ &\alpha_3 := \min\left\{\alpha_2 c_1, \frac{\kappa_2}{2}\right\}, \quad \alpha_4 := \kappa_3\left(1 - \frac{\delta_2}{2}\right) c_2 c_P,\end{aligned}$$

with $c_P > 0$ being the constant in Poincaré's inequality, and δ_1, δ_2 restricted to the ranges indicated in the hypotheses, we find that there exists $\alpha(\Omega) := \min\{\alpha_1, \alpha_3, \alpha_4\}$ such that

$$\mathbf{A}_\phi(\vec{\mathbf{s}}, \vec{\mathbf{s}}) \geq \alpha(\Omega) \| \vec{\mathbf{s}} \|^2 \quad \forall\, \vec{\mathbf{s}} \in \mathcal{H}.$$

On the other hand, using the Cauchy-Schwarz inequality twice, and that $\mathbf{H}^1(\Omega)$ is continuously embedded into $\mathbf{L}^4(\Omega)$ with constant $c_{\mathbf{i}}(\Omega) > 0$, we deduce from (2.22) that

$$-\mathbf{B}_\mathbf{w}(\vec{\mathbf{s}}, \vec{\mathbf{s}}) \leq c_{\mathbf{i}}^2 (1 + \kappa_1^2)^{1/2} \| \mathbf{w} \|_{1,\Omega} \| \vec{\mathbf{s}} \|^2.$$

In this way, putting together the last two equations, we obtain

$$(\mathbf{A}_\phi + \mathbf{B}_\mathbf{w})(\vec{\mathbf{s}}, \vec{\mathbf{s}}) \geq \left(\alpha(\Omega) - c_{\mathbf{i}}^2 (1 + \kappa_1^2)^{1/2} \| \mathbf{w} \|_{1,\Omega}\right) \| \vec{\mathbf{s}} \|^2$$

and therefore

$$(\mathbf{A}_\phi + \mathbf{B}_\mathbf{w})(\vec{\mathbf{s}}, \vec{\mathbf{s}}) \geq \frac{\alpha(\Omega)}{2} \| \vec{\mathbf{s}} \|^2,$$

provided that

$$\| \mathbf{w} \|_{1,\Omega} \leq \frac{\alpha(\Omega)}{2c_{\mathbf{i}}^2 (1 + \kappa_1^2)^{1/2}} =: r_1.$$

□

In turn, as the mixed formulation (2.30) of the energy equation has not changed with respect to the one in [2], we recall the ellipticity result for $\mathbf{C}_\phi + \mathbf{D}_\mathbf{w}$ from [2, Lemma 3.3].

Lemma 2.5 *Assume that for* $\delta_3 \in \left(0, \frac{2}{k_2}\right)$, $\delta_4 \in (0, 2)$ *we choose*

$$\kappa_4 \in \left(0, \frac{2\delta_3 k_1}{k_2}\right), \quad \kappa_5, \kappa_7 \in (0, \infty) \quad \textit{and} \quad \kappa_6 \in \left(0, 2\delta_4 \left(k_1 - \frac{\kappa_4 k_2}{2\delta_3}\right)\right).$$

Then, there exists $r_2 > 0$ *such that for each* $r \in (0, r_2)$, *the bilinear form* $\mathbf{C}_\phi + \mathbf{D}_\mathbf{w}$ *is elliptic in* $\mathcal{Q}$ *for each* $(\mathbf{w}, \phi) \in \mathbf{H}$ *such that* $\| \mathbf{w} \|_{1,\Omega}^2 \leq r$. *More precisely, there exists* $\beta(\Omega) > 0$ *such that*

$$(\mathbf{C}_\phi + \mathbf{D}_\mathbf{w})(\vec{\boldsymbol{\chi}}, \vec{\boldsymbol{\chi}}) \geq \frac{\beta(\Omega)}{2} \| \vec{\boldsymbol{\chi}} \|^2 \quad \forall\, \vec{\boldsymbol{\chi}} \in \mathcal{Q}. \tag{2.34}$$

In this way, for computational purposes, we choose $\delta_1, \delta_2, \kappa_1, \kappa_3, \delta_3, \delta_4, \kappa_4$, and κ_6 as the midpoints of their respective ranges, and take the remaining parameters so as to maximize the computable constants defining $\alpha(\Omega)$ and $\beta(\Omega)$. In this way, we obtain

$$\kappa_1 = \frac{\mu_1}{\mu_2^2}, \quad \kappa_2 = \frac{\mu_1}{\mu_2^2} \quad \kappa_3 = \frac{\mu_1}{2}, \quad \kappa_4 = \frac{k_1}{k_2^2},$$
$$\kappa_5 = \frac{k_1}{2\kappa_2^2}, \quad \kappa_6 = \frac{k_1}{2}, \quad \kappa_7 = \frac{k_1}{4}.$$

Consequently, under the assumptions of Lemmas 2.4 and 2.5, both (2.29) and (2.30) are well-posed problems by means of the Lax–Milgram theorem, and therefore, the operator $\mathbf{T}$ given by (2.31) is well-defined in similar terms as [2, Lemma 3.4]. Then, the analysis of the fixed-point problem can be carried out in the exact same terms as [2, Section 3.4], since we are again benefited by the fact that vorticity does not play a role in these results, and moreover, the aforementioned operators $\mathbf{M}$ and $\mathbf{E}$ coincide with the ones presented in [2]. This leads to (2.32) being a well-posed problem thanks to the Banach fixed-point theorem under some smallness-of-data and suitable regularity assumptions that are not worth mentioning again, for the sake of briefness of this paper. We refer to [2, Theorem 3.9] for further details.

3 Mixed finite element methods

We first present the Galerkin schemes for (2.10) and (2.20) and then specify finite element spaces, based on the flexibility that augmented methods provide. For now, let us consider arbitrary finite dimensional subspaces $\mathbb{H}_h^{\mathbf{t}} \subset \mathbb{L}^2_{\mathtt{tr}}(\Omega)$, $\mathbb{H}_h^{\boldsymbol{\sigma}} \subset \mathbb{H}_0(\mathbf{div};\Omega)$, $\mathbf{H}_h^{\mathbf{u}} \subset \mathbf{H}^1(\Omega)$, $\mathbf{H}_h^{\boldsymbol{\zeta}} \subset \mathbf{L}^2(\Omega)$, $\mathbf{H}_h^{\mathbf{p}} \subset \mathbf{H}_{\mathrm{N}}(\mathrm{div};\Omega)$ and $\mathrm{H}_h^{\varphi} \subset \mathrm{H}^1(\Omega)$, as well as $\mathcal{T}_h$ to be a regular triangulation of $\bar{\Omega}$ made by tetrahedrons T (when $\Omega \subset \mathrm{R}^3$) or triangles T (when $\Omega \subset \mathrm{R}^2$) of diameter h_T and define the meshsize $h := \max\{h_T : T \in \mathcal{T}_h\}$.

3.1 Linear elasticity

Regarding (2.10), the Galerkin scheme reads: Find $(\boldsymbol{\sigma}_h, \mathbf{u}_h) \in \mathbb{H}_h^{\boldsymbol{\sigma}} \times \mathbf{H}_h^{\mathbf{u}}$ such that

$$\mathbf{A}((\boldsymbol{\sigma}_h, \mathbf{u}_h), (\boldsymbol{\tau}_h, \mathbf{v}_h)) = \mathbf{F}(\boldsymbol{\tau}_h, \mathbf{v}_h) \quad \forall\, (\boldsymbol{\tau}_h, \mathbf{v}_h) \in \mathbb{H}_h^{\boldsymbol{\sigma}} \times \mathbf{H}_h^{\mathbf{u}}, \tag{3.1}$$

with $\mathbf{A}$ and $\mathbf{F}$ defined respectively as in (2.11) and (2.12). Following [21], by using the same values for the stabilization parameters as in Lemma 2.2, and since the bilinear form $\mathbf{A}$ is elliptic in $\mathbb{H}_0(\mathbf{div};\Omega) \times \mathbf{H}^1(\Omega)$ (and so it is in $\mathbb{H}_h^{\boldsymbol{\sigma}} \times \mathbf{H}_h^{\mathbf{u}}$), the variational formulation (3.1) is well-posed. Moreover, there exists positive constants C and $\widetilde{C}$, independent of λ and h such that

$$\| (\boldsymbol{\sigma}_h, \mathbf{u}_h) \|_{\mathcal{H}} \leq C \left\{ \| \mathbf{f} \|_{0,\Omega} + \| \mathbf{g} \|_{1/2,\Gamma} \right\}$$

and

$$\| (\boldsymbol{\sigma}, \mathbf{u}) - (\boldsymbol{\sigma}_h, \mathbf{u}_h) \|_{\mathcal{H}} \leq \widetilde{C} \inf_{(\boldsymbol{\tau}_h, \mathbf{v}_h) \in \mathbb{H}_h^{\boldsymbol{\sigma}} \times \mathbf{H}_h^{\mathbf{u}}} \| (\boldsymbol{\sigma}, \mathbf{u}) - (\boldsymbol{\tau}_h, \mathbf{v}_h) \|. \tag{3.2}$$

In addition, since $\boldsymbol{\sigma}$ is certainly symmetric, we can add and subtract $\boldsymbol{\sigma} = \boldsymbol{\sigma}^{\mathtt{t}}$ to obtain

$$\begin{aligned} \left\| \boldsymbol{\sigma}_h - \boldsymbol{\sigma}_h^{\mathtt{t}} \right\|_{0,\Omega} &\leq 2 \| \boldsymbol{\sigma} - \boldsymbol{\sigma}_h \|_{0,\Omega} \leq 2 \| (\boldsymbol{\sigma}, \mathbf{u}) - (\boldsymbol{\sigma}_h, \mathbf{u}_h) \|_{\mathcal{H}} \\ &\leq 2\, \widetilde{C} \inf_{(\boldsymbol{\tau}_h, \mathbf{v}_h) \in \mathbb{H}_h^{\boldsymbol{\sigma}} \times \mathbf{H}_h^{\mathbf{u}}} \| (\boldsymbol{\sigma}, \mathbf{u}) - (\boldsymbol{\tau}_h, \mathbf{v}_h) \|, \end{aligned} \tag{3.3}$$

where the Céa estimate (3.2) has been used in the last inequality.

3.2 Boussinesq problem with temperature-dependent viscosity

Now, considering (2.20), adding a null trace condition to $\mathbf{H}_h^{\mathbf{u}}$, and denoting by

$$\mathcal{H}_h := \mathbb{H}_h^{\mathbf{t}} \times \mathbb{H}_h^{\boldsymbol{\sigma}} \times \mathbf{H}_h^{\mathbf{u}}, \quad \mathcal{Q}_h := \mathbf{H}_h^{\boldsymbol{\zeta}} \times \mathbf{H}_h^{\mathbf{p}} \times \mathrm{H}_h^{\varphi} \tag{3.4}$$

$$\vec{\mathbf{t}}_h := (\mathbf{t}_h, \boldsymbol{\sigma}_h, \mathbf{u}_h), \quad \vec{\mathbf{s}}_h := (\mathbf{s}_h, \boldsymbol{\tau}_h, \mathbf{v}_h), \quad \vec{\boldsymbol{\zeta}}_h := (\boldsymbol{\zeta}_h, \mathbf{p}_h, \varphi_h), \quad \vec{\boldsymbol{\chi}}_h := (\boldsymbol{\chi}_h, \mathbf{q}_h, \psi_h), \tag{3.5}$$

the Galerkin scheme for this problem is given by: Find $(\vec{\mathbf{t}}_h, \vec{\boldsymbol{\zeta}}_h) \in \mathcal{H}_h \times \mathcal{Q}_h$ such that

$$\begin{aligned} \mathbf{A}_{\varphi_h}(\vec{\mathbf{t}}_h, \vec{\mathbf{s}}_h) + \mathbf{B}_{\mathbf{u}_h}(\vec{\mathbf{t}}_h, \vec{\mathbf{s}}_h) &= F_{\varphi_h}(\vec{\mathbf{s}}_h) + F_{\mathrm{m}}(\vec{\mathbf{s}}_h) \qquad \forall\, \vec{\mathbf{s}}_h \in \mathcal{H}_h, \\ \mathbf{C}_{\varphi_h}(\vec{\boldsymbol{\zeta}}_h, \vec{\boldsymbol{\chi}}_h) + \mathbf{D}_{\mathbf{u}_h}(\vec{\boldsymbol{\zeta}}_h, \vec{\boldsymbol{\chi}}_h) &= G_D(\vec{\boldsymbol{\chi}}_h) + G_{\mathrm{e}}(\vec{\boldsymbol{\chi}}_h) \qquad \forall\, \vec{\boldsymbol{\chi}}_h \in \mathcal{Q}_h, \end{aligned} \tag{3.6}$$

where the forms $\mathbf{A}_{\varphi_h}, \mathbf{B}_{\mathbf{u}_h}, \mathbf{C}_{\varphi_h}, \mathbf{D}_{\mathbf{u}_h}$, and the functionals $F_{\varphi_h}, F_{\mathrm{m}}, G_D, G_{\mathrm{e}}$, are defined by (2.21)–(2.28). Following [2], existence of a solution to this problem is guaranteed primarily whenever the stabilization parameters are taken as in Lemmas 2.4 and 2.5 (in order to have ellipticity) and smallness-of-data assumptions like the one presented in [2, Theorem 4.8] hold. In this way, it is possible to prove following [2, Section 4.2] that there exists positive constants $C_{\mathbf{M}}$, $C_{\mathbf{E}}$ such that

$$\| \vec{\mathbf{t}}_h \|_{\mathcal{H}} \leq C_{\mathbf{M}} \left\{ r \| \mathbf{g} \|_{\infty,\Omega} + \| \mathbf{f}^{\mathrm{m}} \|_{0,\Omega} \right\}$$

and

$$\| \vec{\boldsymbol{\zeta}}_h \|_{\mathcal{Q}} \leq C_{\mathbf{E}} \left\{ \| \varphi_D \|_{1/2,\Gamma_D} + \| f^{\mathrm{e}} \|_{0,\Omega} \right\}.$$

Regarding a Céa's estimate for this problem, while it can not be derived as simply as in the Linear Elasticity case, it follows the same scheme as in [2, Section 5]. Once again, vorticity does not play a role in the *a priori* error analysis, as the difference between continuous and discrete forms from Strang's Lemma vanish all but nonlinear terms. Therefore, we conclude that, given data sufficiently small, there exists a constant $\widetilde{C} > 0$ independent of h such that

$$\| (\vec{\mathbf{t}}, \vec{\boldsymbol{\zeta}}) - (\vec{\mathbf{t}}_h, \vec{\boldsymbol{\zeta}}_h) \| \leq \widetilde{C} \left\{ \inf_{\vec{\mathbf{s}}_h \in \mathcal{H}_h} \| \vec{\mathbf{t}} - \vec{\mathbf{s}}_h \|_{\mathcal{H}} + \inf_{\vec{\boldsymbol{\chi}}_h \in \mathcal{Q}_h} \| \vec{\boldsymbol{\zeta}} - \vec{\boldsymbol{\chi}}_h \|_{\mathcal{Q}} \right\}. \tag{3.7}$$

In addition, proceeding exactly as for the derivation of (3.3), we are able to show that

$$\| \boldsymbol{\sigma}_h - \boldsymbol{\sigma}_h^{\mathrm{t}} \|_{0,\Omega} \leq 2\, \widetilde{C} \left\{ \inf_{\vec{\mathbf{s}}_h \in \mathcal{H}_h} \| \vec{\mathbf{t}} - \vec{\mathbf{s}}_h \|_{\mathcal{H}} + \inf_{\vec{\boldsymbol{\chi}}_h \in \mathcal{Q}_h} \| \vec{\boldsymbol{\zeta}} - \vec{\boldsymbol{\chi}}_h \|_{\mathcal{Q}} \right\}. \tag{3.8}$$

3.3 Specification of finite element spaces

It is important to notice that eliminating the vorticity from the system has not imposed any additional restriction on the choice of finite elements, and hence the flexibility on this matter that characterize augmented methods has not been lost. Therefore, we consider these subspaces as in their original works ([2,21]), i.e., given an integer $k \geq 0$,

$$\begin{aligned} \mathbb{H}_h^{\mathbf{t}} &:= \left\{ \mathbf{s}_h \in \mathbb{L}^2_{\mathrm{tr}}(\Omega) : \quad \mathbf{s}_h|_T \in \mathbb{P}_k(T) \quad \forall\, T \in \mathcal{T}_h \right\}, \\ \mathbb{H}_h^{\boldsymbol{\sigma}} &:= \left\{ \boldsymbol{\tau}_h \in \mathbb{H}_0(\mathbf{div}; \Omega) : \quad \mathbf{c}^{\mathrm{t}} \boldsymbol{\tau}_h|_T \in \mathbf{RT}_k(T) \quad \forall\, \mathbf{c} \in \mathrm{R}^2,\ \forall\, T \in \mathcal{T}_h \right\}, \\ \mathbf{H}_h^{\mathbf{u}} &:= \left\{ \mathbf{v}_h \in \mathbf{C}(\bar{\Omega}) : \quad \mathbf{v}_h|_T \in \mathbf{P}_{k+1}(T) \quad \forall\, T \in \mathcal{T}_h \right\}, \end{aligned}$$

$$\mathbf{H}_h^{\boldsymbol{\zeta}} := \Big\{ \boldsymbol{\chi}_h \in \mathbf{L}^2(\Omega) : \quad \boldsymbol{\chi}_h\big|_T \in \mathbf{P}_k(T) \quad \forall\, T \in \mathcal{T}_h \Big\},$$
$$\mathbf{H}_h^{\mathbf{p}} := \Big\{ \mathbf{q}_h \in \mathbf{H}_{\mathrm{N}}(\mathrm{div};\Omega) : \quad \mathbf{q}_h\big|_T \in \mathbf{RT}_k(T) \quad \forall T \in \mathcal{T}_h \Big\},$$
$$\mathrm{H}_h^{\varphi} := \Big\{ \psi_h \in \mathrm{C}(\bar{\Omega}) : \quad \psi_h\big|_T \in \mathrm{P}_{k+1}(T) \quad \forall\, T \in \mathcal{T}_h \Big\},$$

which constitute an approximation of lower cost than those of existing competing schemes for this set of variables. It can be proved that for these spaces, the resulting methods are optimally convergent at a rate $\mathcal{O}(h^{k+1})$ (as long as the exact solutions are sufficiently smooth; see, e.g., [2, Lemma 5.5]). Therefore, according to (3.3) and (3.8), a rate of $\mathcal{O}(h^{k+1})$ can also be expected for the error decay of the symmetry of $\boldsymbol{\sigma}_h$ in both cases. In this way, we realize that the ultra-weak imposition of the symmetry of $\boldsymbol{\sigma}$ does not imply by itself the asymptotic symmetry of the discrete stresses $\boldsymbol{\sigma}_h$, which is actually consequence of the symmetry of $\boldsymbol{\sigma}$ and the corresponding Céa estimate. Nevertheless, it is well known that the latter certainly follows from the ellipticity of the bilinear forms involved, for which, as already emphasized, the use of that imposition is strictly necessary (unless unverifiable conditions on constants and parameters are assumed).

4 Numerical examples

We now present some numerical results that confirm the accuracy of the proposed augmented mixed finite element methods (AMFEM). We also address how the absence of vorticity and the ultra-weak imposition of symmetry influence the quality of approximation. First, we define the individual errors

$$e(\mathbf{t}) := \| \mathbf{t} - \mathbf{t}_h \|_{0,\Omega}, \qquad e(\boldsymbol{\sigma}) := \| \boldsymbol{\sigma} - \boldsymbol{\sigma}_h \|_{\mathbf{div};\Omega}, \qquad e(\mathbf{u}) := \| \mathbf{u} - \mathbf{u}_h \|_{1,\Omega},$$
$$e(\boldsymbol{\zeta}) := \| \boldsymbol{\zeta} - \boldsymbol{\zeta}_h \|_{0,\Omega}, \qquad e(\mathbf{p}) := \| \mathbf{p} - \mathbf{p}_h \|_{\mathrm{div};\Omega}, \qquad e(\varphi) := \| \varphi - \varphi_h \|_{1,\Omega},$$

as well as their corresponding rates of convergence

$$r(\star) := \frac{\log(e(\star)/e'(\star))}{\log(h/h')} \quad \forall\, \star \in \big\{ \mathbf{t}, \boldsymbol{\sigma}, \mathbf{u}, \boldsymbol{\gamma}, \boldsymbol{\zeta}, \mathbf{p}, \varphi \big\},$$

where h and h' denote two consecutive meshsizes with errors e and e'. We also measure the error in the symmetry of the stress tensors as

$$e_{\mathtt{sym}} := \| \boldsymbol{\sigma}_h - \boldsymbol{\sigma}_h^{\mathtt{t}} \|_{0,\Omega}, \quad r_{\mathtt{sym}} := \frac{\log(e_{\mathtt{sym}}/e'_{\mathtt{sym}})}{\log(h/h')}.$$

4.1 Linear elasticity in the nearly incompressible limit

In this section we conduct numerical experiments similarly to those in [21, Tests 1 & 2]. Both problems involve three-dimensional domains, and given the Young modulus

$E = 1$ and a Poisson ratio ν, we consider the following Lamé parameters:

$$\mu := \frac{E}{2(1+\nu)} \quad \text{and} \quad \lambda := \frac{E\,\nu}{(1+\nu)(1-2\nu)}.$$

Example 1 First, we set $\Omega = (0,1)^3$, $\nu = 0.4900$ (that is, $\mu = 0.3356$ and $\lambda = 16.4430$) and source terms such that a closed-form solution to (2.4) is given by

$$\boldsymbol{\sigma} = \mathscr{C}\mathbf{e}(\mathbf{u}), \quad \mathbf{u} = \ell(x^2+1)(y^2+1)(z^2+1)\exp(x+y+z)\begin{pmatrix}1\\1\\1\end{pmatrix},$$

with $\ell = 0.04$. Note that the exact stress does not satisfy the condition $\int_\Omega \operatorname{tr}(\boldsymbol{\sigma}) = 0$. Nevertheless, here and in all subsequent tests, we can impose the condition $\int_\Omega \operatorname{tr}(\boldsymbol{\sigma}) = \int_\Omega \operatorname{tr}(\boldsymbol{\sigma}_{\text{exact}})$ by means of a real Lagrange multiplier (accounting for augmenting the resulting linear systems with one row and one column), see e.g. [21, Eq. (4.11)].

Example 2 We next focus on the three-dimensional L-shaped domain $\Omega = (-0.5, 0.5)\times(0,1)\times(-0.5,0.5)\backslash\big\{(0,0.5)\times(0,1)\times(0,0.5)\big\}$, $\nu = 0.4999$ (giving $\mu = 0.3333$ and $\lambda = 1666.4444$) and define source terms such that the exact solution to (2.4) is the Kelvin fundamental solution

$$\boldsymbol{\sigma} = \mathscr{C}\mathbf{e}(\mathbf{u}), \quad \mathbf{u} = \frac{A}{r^3}\begin{pmatrix}(x-0.25)^2\\(x-0.25)(y-0.5)\\(x-0.25)(z-0.25)\end{pmatrix} + \frac{B}{r}\begin{pmatrix}1\\0\\0\end{pmatrix},$$

where $A = \frac{1}{16\pi\mu(1-\nu)}$, $B = \frac{3-4\nu}{16\pi\mu(1-\nu)}$ and $r = \big[(x-0.25)^2 + (y-0.5)^2 + (z-0.25)^2\big]^{1/2}$.

We show in Tables 1 and 2 a convergence history on a set of quasi-uniform refinements for each of the exact aforementioned solutions. Since these are smooth, the AMFEM with ultra-weakly imposed symmetry converges at $\mathcal{O}(h^{k+1})$ (as expected from the previous section) when the finite element $(\mathbb{H}_h^{\boldsymbol{\sigma}}, \mathbf{H}_h^{\mathbf{u}})$ from Sect. 3.3 is used. Moreover, as the vorticity has been removed from the system, the overall rate of convergence (dictated by the decay of the stress error) is slightly higher than in [21] (see also Table 3, below). Sample solutions are provided in Fig. 1, where we can see that the off-diagonal components of the Cauchy stress practically coincide. The same behavior occurs for Example 2, as evidenced in Fig. 2.

Perhaps one of the key differences of this method with respect to [21] is the reduction in degrees of freedom (DOF) and how symmetric the stress tensor is. Since the skew-symmetric vorticity tensor can be fully described with only 3 components, the reduction in 3 DOFs per element (when using a approximation by piecewise constant polynomials) with respect to the method in [21] is clear. This is confirmed further by portraying on Table 3 DOFs and symmetry errors associated with the method from [21] (focusing again on Example 1). The ultra-weak imposition leads to a comparable symmetry error (by observing again the values from the top block of Table 1), and both errors decay with $\mathcal{O}(h^{k+1})$, as expected.

Table 1 Example 1. Error history for the vorticity-free AMFEM using first and second-order approximations

DOF	h	$e(\boldsymbol{\sigma})$	$r(\boldsymbol{\sigma})$	$e(\mathbf{u})$	$r(\mathbf{u})$	$e_{\mathtt{sym}}$	$r_{\mathtt{sym}}$
$k=0$							
2968	0.4332	7.7342	–	1.253	–	0.2226	–
9454	0.2887	5.2691	0.9464	0.7196	1.3672	0.1416	1.1162
21,772	0.2165	3.9773	0.9781	0.4798	1.4090	0.1043	1.0630
41,794	0.1732	3.1897	0.9897	0.3487	1.4319	0.0810	1.1314
71,392	0.1443	2.6642	0.9949	0.2695	1.4134	0.0651	1.1946
112,438	0.1237	2.2810	0.9975	0.2186	1.3561	0.0538	1.2447
166,804	0.1083	1.9962	0.9988	0.1847	1.2651	0.0453	1.2835
236,362	0.0962	1.7744	0.9996	0.1613	1.1487	0.0384	1.3145
$k=1$							
13,420	0.4332	0.3036	–	0.1771	–	0.1286	–
43,528	0.2887	0.1441	1.8333	0.1132	1.3103	0.0676	1.6584
101,140	0.2165	0.0847	1.8457	0.0018	1.5675	0.0415	1.7697
195,184	0.1732	0.0384	1.9832	0.0003	1.9431	0.0153	1.9138
334,588	0.1443	0.0110	1.9906	0.0001	1.8795	0.0044	1.9581

Table 2 Example 2. Decay of the Cauchy stress, displacement, and symmetry errors produced by the vorticity-free AMFEM with first and second-order approximations

DOF	h	$e(\boldsymbol{\sigma})$	$r(\boldsymbol{\sigma})$	$e(\mathbf{u})$	$r(\mathbf{u})$	$e_{\mathtt{sym}}$	$r_{\mathtt{sym}}$
$k=0$							
2530	0.5349	1.0631	–	0.7136	–	0.7811	–
4600	0.3685	0.3228	1.8539	0.3452	1.9428	0.2514	1.8042
11,995	0.2625	0.1519	1.2443	0.2359	1.1238	0.1566	1.2396
24,265	0.1991	0.1143	1.0083	0.1908	0.8662	0.1154	1.1042
45,655	0.1639	0.0931	1.0485	0.1613	0.9661	0.0956	0.9655
73,876	0.1382	0.0763	1.1671	0.1357	1.0140	0.0774	1.1239
113,146	0.1207	0.0665	1.0115	0.1205	0.9737	0.0679	0.9712
$k=1$							
11,194	0.5349	0.5322	–	0.4926	–	0.4788	–
20,932	0.3685	0.1168	1.7591	0.2163	1.8482	0.2112	1.9271
55,258	0.2625	0.0387	1.8568	0.0585	1.8956	0.0557	2.1343
112,882	0.1991	0.0172	1.9443	0.0268	2.0819	0.0219	2.1108
213,274	0.1639	0.0108	2.0386	0.0182	1.9860	0.0133	2.0493

4.2 The Boussinesq problem in two and three dimensions

We now turn to the numerical verification of the properties of the vorticity-free AMFEM presented in (3.6). We follow the experiments in [2] to show that this new method provides comparable results, at a lower computational cost.

Table 3 Error history for the lowest-order augmented FEM from [21]. Here m is the number of tetrahedra in each mesh. The quantities without tildes denote DOFs and ratios associated with the proposed vorticity-free AMFEM. The reduction in 3 DOFs per element is clear

$\widetilde{\text{DOF}}$	DOF	m	$\widetilde{\text{DOF}}/m$	DOF/m	$\widetilde{e(\boldsymbol{\sigma})}$	$\widetilde{r(\boldsymbol{\sigma})}$	$\widetilde{e_{\mathtt{sym}}}$	$\widetilde{r_{\mathtt{sym}}}$
4120	2968	384	10.73	7.721	7.7932	–	0.9664	–
13,342	9454	1296	10.29	7.294	5.4342	0.891	0.7213	0.8305
30,988	21,772	3072	10.09	7.087	4.0173	1.048	0.5056	1.0343
59,794	41,794	6000	9.962	6.996	3.2033	1.015	0.2835	1.0593
102,496	71,392	10,368	9.881	6.892	2.6674	1.004	0.1563	1.1235

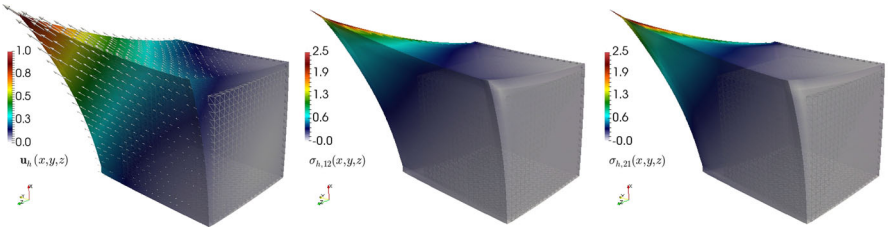

Fig. 1 Example 1. Velocity magnitude plotted on the deformed configuration, and XY–YX components of the Cauchy stress. The skeleton mesh is displayed on the undeformed geometry

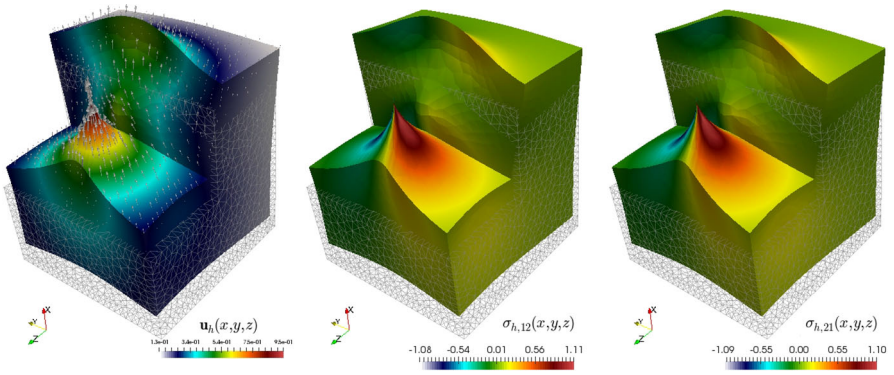

Fig. 2 Example 2. Velocity magnitude plotted on the deformed configuration, and XY–YX components of the Cauchy stress. The skeleton mesh is displayed on the undeformed geometry

Example 3 Here, $\Omega = (-1,1)^2$, $\Gamma_D = [-1,1] \times \{-1,1\}$, $\Gamma_N = \Gamma \backslash \Gamma_D$, and we consider viscosity, thermal conductivity and body force as

$$\mu(\varphi) = \exp(-0.25\,\varphi), \quad k(\varphi) = \exp(0.25\,\varphi), \quad \mathbf{g} = (0,1)^{\mathtt{t}},$$

where source terms $\mathbf{f}^{\mathtt{m}}$, $\mathbf{f}^{\mathtt{e}}$ and boundary conditions are prescribed in such a way that the exact solution to (2.16) is given by

Table 4 Example 3. Convergence history and Picard iteration count for the vorticity-free AMFEM applied to the Boussinesq equations in 2D

Augmented mixed method with $k = 0$								
DOF	h	$e(\mathbf{t})$	$e(\boldsymbol{\sigma})$	$e(\mathbf{u})$	$e(\boldsymbol{\zeta})$	$e(\mathbf{p})$	$e(\varphi)$	$e_{\mathtt{sym}}$
108	1.4140	12.872	43.892	19.922	3.3349	5.7051	5.8226	6.3685
372	0.7071	9.0262	29.189	16.431	1.7892	5.6377	4.4035	4.1118
1380	0.3536	5.6625	17.016	10.832	1.1887	4.5898	2.7744	3.8566
5316	0.1768	3.1263	8.8880	5.4914	0.5501	2.6782	1.5790	2.1146
20,868	0.0884	1.5659	4.5021	2.6512	0.2438	1.3671	0.8343	1.0861
82,692	0.0442	0.7779	2.2675	1.2996	0.1159	0.6783	0.4301	0.5337
329,220	0.0221	0.3875	1.1313	0.6437	0.0570	0.3376	0.2184	0.2513
iter	$r(\mathbf{t})$	$r(\boldsymbol{\sigma})$	$r(\mathbf{u})$	$r(\boldsymbol{\zeta})$	$r(\mathbf{p})$	$r(\varphi)$	$r_{\mathtt{sym}}$	
10	–	–	–	–	–	–	–	
10	0.5117	0.5929	0.2792	0.8983	0.0162	0.4123	0.4845	
10	0.6727	0.7746	0.6012	0.5901	0.2946	0.6667	0.6645	
10	0.8568	0.9365	0.9785	1.1114	0.7829	0.8216	0.8654	
9	0.9986	0.9811	1.0527	1.1748	0.9731	0.9117	0.9691	
9	1.0081	0.9945	1.0296	1.0727	1.0091	0.9559	1.0138	
9	1.0053	0.9982	1.0146	1.0223	1.0074	0.9781	1.0354	
Augmented mixed method with $k = 1$								
DOF	h	$e(\mathbf{t})$	$e(\boldsymbol{\sigma})$	$e(\mathbf{u})$	$e(\boldsymbol{\zeta})$	$e(\mathbf{p})$	$e(\varphi)$	$e_{\mathtt{sym}}$
316	1.4140	7.258	19.74	11.48	1.312	2.93	3.045	4.891
1156	0.7071	2.341	6.231	4.767	0.4386	1.69	1.143	1.751
4420	0.3536	0.662	1.702	1.355	0.1413	0.3992	0.2598	0.69
17,284	0.1768	0.1781	0.4442	0.3534	0.03768	0.1014	0.06594	0.2064
68,356	0.0884	0.04578	0.1128	0.08921	0.009655	0.02574	0.01676	0.05545
271,876	0.0442	0.01156	0.02881	0.02237	0.00244	0.006488	0.00423	0.01417
iter	$r(\mathbf{t})$	$r(\boldsymbol{\sigma})$	$r(\mathbf{u})$	$r(\boldsymbol{\zeta})$	$r(\mathbf{p})$	$r(\varphi)$	$r_{\mathtt{sym}}$	
9	–	–	–	–	–	–	–	
9	1.6325	1.6649	1.2683	1.5818	0.7938	1.4147	1.4852	
9	1.8228	1.8726	1.8159	1.6343	2.0822	2.1373	1.6453	
9	1.8949	1.9383	1.9396	1.9072	1.9774	1.9781	1.7421	
9	1.9656	1.9784	1.9861	1.9659	1.9797	1.9765	1.8966	
9	1.9867	1.9693	1.9954	1.9857	1.9889	1.9860	1.9648	

$$\mathbf{u} = \begin{pmatrix} 2y\sin(\pi x)\sin(\pi y)(x^2-1) + \pi\sin(\pi x)\cos(\pi y)(x^2-1)(y^2-1) \\ -2x\sin(\pi x)\sin(\pi y)(y^2-1) - \pi\cos(\pi x)\sin(\pi y)(x^2-1)(y^2-1), \end{pmatrix},$$
$$\mathbf{t} = \mathbf{e}(\mathbf{u}),$$
$$\varphi = -0.6944\, y^4 + 1.6944\, y^2, \quad \boldsymbol{\sigma} = \mu(\varphi)\mathbf{t} - \mathbf{u}\otimes\mathbf{u} - (y^2 - x^2)\mathbb{I}, \quad \boldsymbol{\zeta} = \nabla\varphi,$$
$$\mathbf{p} = k(\varphi)\boldsymbol{\zeta} - \varphi\mathbf{u}.$$

Table 5 Example 4. Convergence history and Picard iteration count for the vorticity-free AMFEM applied to the Boussinesq equations in 3D

Augmented mixed method with $k = 0$								
DOF	h	$e(\mathbf{t})$	$e(\boldsymbol{\sigma})$	$e(\mathbf{u})$	$e(\boldsymbol{\zeta})$	$e(\mathbf{p})$	$e(\varphi)$	$e_{\mathtt{sym}}$
153	1.0322	0.4303	5.5768	0.2308	0.8549	22.737	6.0623	0.7802
3065	0.5774	0.1128	2.2324	0.1479	2.5377	11.8923	2.3667	7.5091
13,465	0.3464	0.0383	1.0762	0.0356	0.7871	7.2175	1.2359	0.0604
36,153	0.2474	0.0161	0.8179	0.0184	0.3587	5.2149	0.8593	0.0359
75,929	0.1925	0.0100	0.6477	0.0132	0.2661	4.0870	0.6752	0.0256
137,593	0.1575	0.0073	0.5341	0.0105	0.2203	3.3563	0.5573	0.0199
225,945	0.1332	0.0057	0.4538	0.0088	0.1911	2.8454	0.4749	0.0104
345,785	0.1155	0.0047	0.3942	0.0076	0.1701	2.4687	0.4142	0.0139
501,913	0.1019	0.0041	0.3483	0.0064	0.1541	2.1831	0.3675	0.0120
`iter`	$r(\mathbf{t})$	$r(\boldsymbol{\sigma})$	$r(\mathbf{u})$	$r(\boldsymbol{\zeta})$	$r(\mathbf{p})$	$r(\varphi)$	$r_{\mathtt{sym}}$	
7	–	–	–	–	–	–	–	
7	1.1419	0.7961	1.3655	1.0357	0.8846	0.9162	0.6386	
8	1.2462	1.0832	1.8490	1.2681	1.2127	1.7091	0.8981	
8	1.3583	0.8156	1.2549	1.2359	0.9647	1.0824	1.2549	
8	1.2885	0.9291	1.3245	1.1892	0.9626	0.9600	1.2342	
7	1.2587	0.9607	1.1323	0.9408	0.9812	0.9571	1.1253	
7	1.2141	0.9757	1.0550	0.8517	0.9873	0.9569	1.1187	
7	1.1292	0.9843	1.0234	0.9109	0.9907	0.9566	1.1420	
7	1.1208	0.9891	1.0025	0.9899	0.9929	0.956	1.1103	
Augmented mixed method with $k = 1$								
DOF	h	$e(\mathbf{t})$	$e(\boldsymbol{\sigma})$	$e(\mathbf{u})$	$e(\boldsymbol{\zeta})$	$e(\mathbf{p})$	$e(\varphi)$	$e_{\mathtt{sym}}$
589	1.7326	0.0262	5.7147	0.0310	0.9276	1.3559	1.0891	0.0004
13,037	0.5774	0.0074	0.1622	0.0078	0.2089	0.7459	0.2749	0.0144
58,125	0.3464	0.0018	0.0553	0.0033	0.0738	0.2571	0.1011	0.0058
156,973	0.2474	0.0007	0.0208	0.0019	0.0358	0.1225	0.0487	0.0031
330,701	0.1925	0.0003	0.0095	0.0011	0.0194	0.0664	0.0283	0.0019
600,429	0.1575	0.0001	0.0050	0.0005	0.0125	0.0430	0.0185	0.0011
`iter`	$r(\mathbf{t})$	$r(\boldsymbol{\sigma})$	$r(\mathbf{u})$	$r(\boldsymbol{\zeta})$	$r(\mathbf{p})$	$r(\varphi)$	$r_{\mathtt{sym}}$	
8	–	–	–	–	–	–	–	
8	1.9271	2.2042	1.6473	1.8357	2.2497	1.7923	1.7149	
9	1.7696	2.1048	1.6910	2.0336	2.0835	1.9583	1.7736	
9	1.9068	2.1901	1.8399	2.1424	2.1204	2.1638	1.8535	
9	1.9454	2.1315	1.8937	2.4472	2.1432	2.1664	1.8969	
8	1.9530	2.1081	1.9182	2.1891	2.1650	2.0925	1.9253	

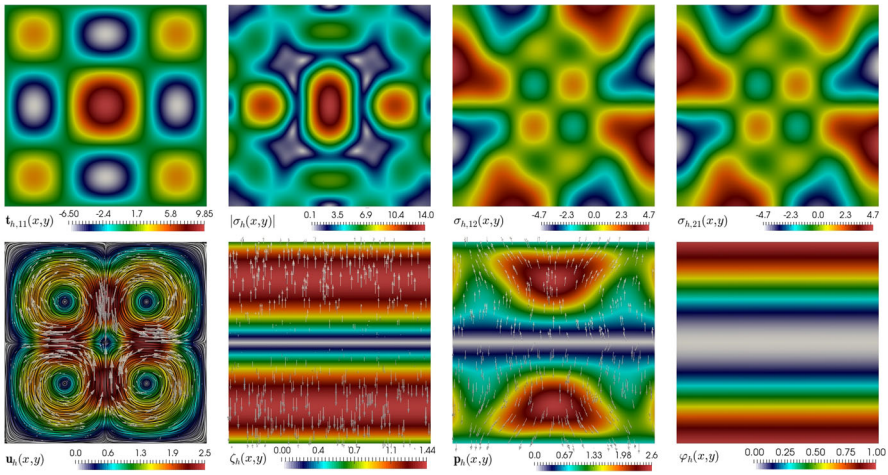

Fig. 3 Example 3. XX component of the strain rate, pseudostress magnitude, XY and YX components of the pseudostress, velocity, temperature gradient, total heat flux, and temperature, computed with a first-order scheme associated with 68,356 DOF

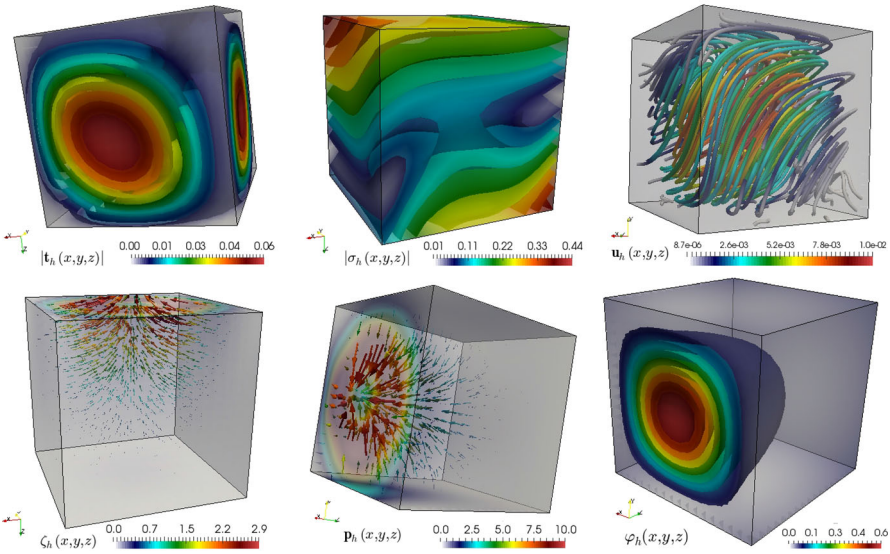

Fig. 4 Example 4. Strain rate magnitude, pseudostress magnitude, velocity streamlines, temperature gradient, total flux, and temperature, computed with a first-order scheme associated with 345,785 DOF

In addition, bounds for the physical properties are estimated in $\mu_1 = 0.5$, $\mu_2 = 1.25$, $k_1 = 0.75$ and $k_2 = 1.3$ and the Picard algorithm starts with $(\mathbf{u}, \varphi) = (\mathbf{0}, 0)$.

Example 4 Finally, we consider $\Omega = (0,1)^3$, $\Gamma_D = [0,1]^2 \times \{0\}$, $\Gamma_N = \Gamma \backslash \Gamma_D$, viscosity, thermal conductivity and body force as

$$\mu(\varphi) = 2.0 - 0.5\,\varphi^2 - 0.5\,\varphi^4, \quad k(\varphi) = -0.5 + 2.0\,\mu(\varphi), \quad \mathbf{g} = (0, 0, 1)^{\mathrm{t}},$$

and source terms and boundary conditions such that the exact solution is given by

$$\mathbf{u} = \begin{pmatrix} 8x^2yz(x-1)^2(y-1)(z-1)(y-z) \\ -8xy^2z(x-1)(y-1)^2(z-1)(x-z) \\ 8xyz^2(x-1)(y-1)(z-1)^2(x-y), \end{pmatrix}, \quad \varphi = \sin(\pi x)^2 \sin(\pi y)^2 (z-1)^2,$$

$$\mathbf{t} = \mathbf{e}(\mathbf{u}), \quad \boldsymbol{\sigma} = \mu(\varphi)\mathbf{t} - \mathbf{u} \otimes \mathbf{u} - (x - 0.5)^3 \sin(y + z)\mathbb{I},$$
$$\boldsymbol{\zeta} = \nabla\varphi, \quad \mathbf{p} = k(\varphi)\boldsymbol{\zeta} - \varphi\mathbf{u}.$$

The bounds for the physical properties are estimated in this case as $\mu_1 = 1.0, \mu_2 = 2.0$, $k_1 = 1.5$ and $k_2 = 3.5$, and the Picard algorithm starts with $(\mathbf{u}, \varphi) = (\mathbf{0}, 0)$.

In Tables 4 and 5 we can observe that when using the finite element ($\mathbb{H}^{\mathbf{t}}_h$, $\mathbb{H}^{\boldsymbol{\sigma}}_h$, $\mathbf{H}^{\mathbf{u}}_h$, $\mathbf{H}^{\boldsymbol{\zeta}}_h$, $\mathbf{H}^{\mathbf{p}}_h$, H^{φ}_h) from Sect. 3.3 with $k = 0$ and $k = 1$, the vorticity-free AMFEM converges at a rate $\mathcal{O}(h^{k+1})$. The reduction in DOF for this scheme is clear, but more importantly, it can also be seen that this does not lead to an increase of fixed-point iterations. Similarly to [2], a solution with a tolerance of 10^{-8} can be achieved for these problems in less than 10 Picard steps. Sample solutions for Examples 3 and 4 are displayed in Figs. 3 and 4.

References

1. Adams, S., Cockburn, B.: A mixed finite element for elasticity in three dimensions. J. Sci. Comput. **25**, 515–521 (2005)
2. Almonacid, J.A., Gatica, G.N.: A fully-mixed finite element method for the Boussinesq problem with temperature-dependent parameters. Comput. Methods Appl. Math. (2019). https://doi.org/10.1515/cmam-2018-0187
3. Almonacid, J.A., Gatica, G.N., Oyarzúa, R.: A mixed-primal finite element method for the Boussinesq problem with temperature-dependent viscosity. Calcolo **55**(3), 36 (2018)
4. Almonacid, J.A., Gatica, G.N., Oyarzúa, R., Ruiz-Baier, R.: A new mixed finite element method for the n-dimensional Boussinesq problem with temperature-dependent viscosity. Preprint 2018–18, Centro de Investigacion en Ingenieria Matematica (CI^{2}MA). Universidad de Concepcion, Chile (2018)
5. Alvarez, M., Gatica, G.N., Gomez-Vargas, B., Ruiz-Baier, R.: New mixed finite element methods for natural convection with phase-change in porous media. J. Sci. Comput. **80**(1), 141–174 (2019)
6. Arnold, D.N., Brezzi, F., Douglas, J.: PEERS: a new mixed finite element for plane elasticity. Japan J. Appl. Math. **1**, 347–367 (1984)
7. Arnold, D.N., Falk, R.S., Winther, R.: Differential complexes and stability of finite element methods. II. The elasticity complex. In: Arnold, D.N., Bochev, P.B., Lehoucq, R.B., Nicolaides, R.A., Shashkov, M. (eds.) Compatible Spatial Discretizations. IMA Vol. Math. Appl., vol. 142, pp. 47–67. Springer, New York (2006)
8. Arnold, D.N., Falk, R.S., Winther, R.: Finite element exterior calculus, homological techniques, and applications. Acta Numer. **15**, 1–155 (2006)
9. Arnold, D.N., Falk, R.S., Winther, R.: Mixed finite element methods for linear elasticity with weakly imposed symmetry. Math. Comput. **76**(260), 1699–1723 (2007)
10. Arnold, D.N., Winther, R.: Mixed finite elements for elasticity. Numer. Math. **92**(3), 401–419 (2002)
11. Artioli, E., de Miranda, S., Lovadina, C., Patruno, L.: A stress/displacement virtual element method for plane elasticity problems. Comput. Methods Appl. Mech. Eng. **325**, 155–174 (2017)
12. Artioli, E., de Miranda, S., Lovadina, C., Patruno, L.: A family of virtual element methods for plane elasticity problems based on the Hellinger–Reissner principle. Comput. Methods Appl. Mech. Eng. **340**, 978–999 (2018)

13. Boffi, D., Brezzi, F., Fortin, M.: Reduced symmetry elements in linear elasticity. Comm. Pure Appl. Anal. **8**, 1–28 (2009)
14. Camaño, J., Oyarzúa, R., Ruiz-Baier, R., Tierra, G.: Error analysis of an augmented mixed method for the Navier–Stokes problem with mixed boundary conditions. IMA J. Numer. Anal. **38**(3), 1452–1484 (2018)
15. Colmenares, E., Gatica, G.N., Oyarzúa, R.: Analysis of an augmented mixed-primal formulation for the stationary Boussinesq problem. Numer. Methods Partial Differ. Equ. **32**(2), 445–478 (2016)
16. Colmenares, E., Gatica, G.N., Oyarzúa, R.: An augmented fully-mixed finite element method for the stationary Boussinesq problem. Calcolo **54**(1), 167–205 (2017)
17. Fraejis de Veubeke, B.X.: Stress function approach. In: World Congress on the Finite Element Method in Structural Mechanics, Bournemouth (1975)
18. Gatica, G.N.: Analysis of a new augmented mixed finite element method for linear elasticity allowing $\mathbb{RT}_0 - \mathbb{P}_1 - \mathbb{P}_0$ approximations, M2AN Math. Model. Numer. Anal. **40**(1), 1–28 (2006)
19. Gatica, G.N.: An augmented mixed finite element method for linear elasticity with non-homogeneous Dirichlet conditions. Electron. Trans. Numer. Anal. **26**, 421–438 (2007)
20. Gatica, G.N.: A Simple Introduction to the Mixed Finite Element Method: Theory and Applications. Springer Briefs in Mathematics. Springer, Cham (2014)
21. Gatica, G.N., Márquez, A., Meddahi, S.: An augmented mixed finite element method for 3D linear elasticity problems. J. Comput. Appl. Math. **231**(2), 526–540 (2009)
22. McLean, W.: Strongly Elliptic Systems and Boundary Integral Equations. Cambridge University Press, New York (2000)
23. Pechstein, A., Schöberl, J.: Tangential-displacement and normal–normal-stress continuous mixed finite elements for elasticity. Math. Models Methods Appl. Sci. **21**(8), 1761–1782 (2011)
24. Pechstein, A., Schöberl, J.: An analysis of the TDNNS method using natural norms. Numer. Math. **139**(1), 93–120 (2018)
25. Stenberg, R.: A family of mixed finite element methods for the elasticity problem. Numer. Math. **53**, 513–538 (1988)

Affiliations

Javier A. Almonacid[1,2] · Gabriel N. Gatica[3] · Ricardo Ruiz-Baier[4,5]

Javier A. Almonacid
jalmonacid@ci2ma.udec.cl; javiera@sfu.ca

Ricardo Ruiz-Baier
ruizbaier@maths.ox.ac.uk

1 Centro de Investigación en Ingeniería Matemática (CI^{2}MA), Universidad de Concepción, Casilla 160-C, Concepción, Chile

2 Present Address: Department of Mathematics, Simon Fraser University, 8888 University Drive, Burnaby, BC V5A 1S6, Canada

3 CI^{2}MA and Departamento de Ingeniería Matemática, Universidad de Concepción, Casilla 160-C, Concepción, Chile

4 Mathematical Institute, University of Oxford, Woodstock Road, Oxford OX2 6GG, UK

5 Present Address: School of Mathematical Sciences, Monash University, 9 Rainforest walk, Clayton, VIC 3800, Australia